December 2000 • NREL/SR-520-29288

Subcontractor Report

Efficiency and Throughput Advances in Continuous Roll-to-Roll a-Si Alloy PV Manufacturing Technology

Phase II Annual Subcontract Technical Report June 1999—August 2000

T. Ellison
Energy Conversion Devices, Inc.
Troy, Michigan

National Renewable Energy Laboratory

1617 Cole Boulevard
Golden, Colorado 80401-3393

NREL is a U.S. Department of Energy Laboratory
Operated by Midwest Research Institute • Battelle • Bechtel

Contract No. DE-AC36-99-GO10337

December 2000 • NREL/SR-520-29288

Efficiency and Throughput Advances in Continuous Roll-to-Roll a-Si Alloy PV Manufacturing Technology

Phase II Annual Subcontract Technical Report June 1999—August 2000

T. Ellison
Energy Conversion Devices, Inc.
Troy, Michigan

NREL Technical Monitor: R.L. Mitchell

Prepared under Subcontract No. ZAX-8-17647-09

National Renewable Energy Laboratory

1617 Cole Boulevard
Golden, Colorado 80401-3393

NREL is a U.S. Department of Energy Laboratory
Operated by Midwest Research Institute • Battelle • Bechtel

Contract No. DE-AC36-99-GO10337

NOTICE

Available electronically at http://www.doe.gov/bridge

Available for a processing fee to U.S. Department of Energy
and its contractors, in paper, from:

U.S. Department of Energy
Office of Scientific and Technical Information
P.O. Box 62
Oak Ridge, TN 37831-0062
phone: 865.576.8401
fax: 865.576.5728
email: reports@adonis.osti.gov

Available for sale to the public, in paper, from:

U.S. Department of Commerce
National Technical Information Service
5285 Port Royal Road
Springfield, VA 22161
phone: 800.553.6847
fax: 703.605.6900
email: orders@ntis.fedworld.gov
online ordering: http://www.ntis.gov/ordering.htm

Printed on paper containing at least 50% wastepaper, including 20% postconsumer waste

TABLE OF CONTENTS

TABLE OF CONTENTS (cont.)

LIST OF FIGURES

LIST OF TABLES

SUMMARY

Introduction

Energy Conversion Devices, Inc. (ECD) and its American joint venture, United Solar Systems Corp. (United Solar), have developed and commercialized a roll-to-roll triple junction amorphous silicon alloy PV manufacturing technology. This low material cost, roll-to-roll production technology has the economies of scale to needed meet the cost goals necessary for widespread use of PV. ECD developed and built the present 5 MW United Solar manufacturing plant in Troy, Michigan, and is now designing and building a new 25 MW facility, also in Michigan. United Solar holds the world's record for amorphous silicon PV conversion efficiency, and manufactures and markets a wide range of PV products including flexible portable modules, power modules, and innovative Building Integrated PV (BIPV) shingle and metal roofing modules that take advantage of this lightweight, rugged and flexible PV technology. All of United Solar's power and BIPV products are U.L. approved and carry a 10-year warrantee.

In this PVMaT 5A subcontract, ECD and United Solar are addressing issues to reduce the cost and improve the manufacturing technology for the ECD/United Solar PV module manufacturing process. ECD and United Solar identified five technology development tasks that would reduce the module manufacturing cost in the present 5 MW production facility, and also be applicable to future larger scale manufacturing facilities. These development tasks are:

Task 5: Improved substrate heating and monitoring systems;
Task 6: The development of new on-line diagnostic systems;
Task 7: Development of new backreflector deposition technology;
Task 8: Development of improved rf PECVD reactor cathode and gas distribution configurations; and
Task 8A: Development of new pinch valve technology

All these tasks are proving to be remarkably successful in terms of:

1. Meeting the goals and milestones of the program;
2. implementing the new technology in the present 5 MW United Solar production equipment with tangible benefits; and also
3. incorporating these new technologies into the design of the new United Solar 25 MW production equipment now being fabricated by ECD.

In the following section we provide a brief overview of these tasks. In subsequent sections these tasks are discussed individually in more detail.

Personnel

The following people at ECD and United Solar have contributed to this project:

Energy Conversion Devices, Inc.

Gennady Bondarenko	PV Deposition Engineer
Joe Doehler	Senior Scientist
Tim Ellison	Senior Scientist, PI
Masat Izu	Former PI, VP Film Technology; presently CEO of the Overhead Door Company)
Scott Jones	Senior Scientist
Mark Lycette	Senior Process Engineer
Art Myatt	PV Engineer/Technical Writer
Herb Ovshinsky	Director of Machine Division

United Solar Systems Corp.

Arindam Banerjee	Director of R&D
Jon Call	Quality Assurance Manager
Subhendu Guha	President
Kevin Hoffman	Director of Production
Jeff Yang	V.P. R&D
Mike Walters	QA Engineer

OVERVIEW OF THE FIVE DEVELOPMENT TASKS

Task 5 – Process Control Improvements: Substrate Heating and Temperature Monitoring Systems

ECD has traditionally used quartz envelope infrared (IR) lamps to heat the substrate in the amorphous silicon deposition machines. These lamps, because they run hot, would get coated along with the substrate. The accumulation of deposition material on these lamps, in combination with the temperature cycling, resulted in flaking of deposition material and in physical stresses that would break the lamps' quartz envelopes. Breakage during runs was minimized by routine changing of the lamps every couple of months.

In this program we proposed replacing these infrared heaters with low-temperature, long-lasting NiChrome (Nickel Chrome alloy) resistance heaters. A system was designed, tested, optimized and proven in United Solar's 2 MW pilot production line. An improved system was then designed, fabricated, and installed in the 5 MW production equipment. The original set of heaters installed in the system, after an initial modification to improve the ceramic insulators, are still functioning after about 500 production runs. Although there have been a few isolated failures, and the heater elements have lost some of their malleability, we still have not determined their lifetime. They appear to be "self-cleaning", and are extremely robust.

The substrate heating system is no longer a significant source of machine downtime due to lamp failure. The new lamps have also eliminated a major maintenance item: the IR lamps had to be replaced about every nine weeks; the material cost was about 24 k$, and this maintenance operation took about 20 hrs. We estimate that these new lamps, which have a lifetime of at least a couple of years, reduce our manufacturing cost by about 0.06 $/W.

In the process of optimizing these new heaters, we have also developed a technique to decrease the crossweb temperature non-uniformity by more than an order of magnitude. This new substrate heating system is now serving as a model for the heating and temperature monitoring systems being designed for the new 25 MW production equipment that ECD is building for United Solar. All the program goals and milestones for this task have been met, most ahead of schedule.

Task 6: In-Line Sensors

Online diagnostic systems can improve the manufacturing process in several ways: they can immediately alert operators to changes in the output of a process, increase the process optimization feedback rate by orders of magnitude compared to off-line QA/QC, and provide the potential for expert system process control and optimization. These capabilities can also reduce the time needed for commissioning new equipment.

In the Phase II portion of this project we have focussed our work on 3 diagnostic systems: a scatterometer and ZnO thickness monitor for the backreflector (BR) machine, and a PV Capacitive Diagnostic (PVCD) system for the amorphous silicon machine.

In the Phase I portion of this program, the hardware systems were developed and tested on the bench, and new second generation systems were designed for installation in the deposition equipment vacuum systems. In the Phase II portion of the program we tested the ZnO thickness monitor and second generation PVCD in the production machines in a production environment; the second generation scatterometer was fabricated and is undergoing bench testing, and the third generation PVCD was specified, designed, and fabricated for bench testing.

The BR Scatterometer:

The first version fabricated and bench tested in Phase I used a fixed laser and a photo-detector on a moving arm to measure both the specular and diffuse reflectance. This device allowed us to determine which angles are of interest and to begin to correlate reflectivity vs. angle measurements with device quality. In Phase II a second generation system was then built for installation in the 5 MW BR machine. This device has no moving parts, and has all the electronics mounted external to the vacuum system. It uses a fixed laser, a photo-diode for measuring the specular component and a photo-diode array to measure the diffuse reflectance. This system is presently undergoing bench testing.

BR Thickness Monitor

The BR thickness monitor is installed in the production BR machine and is in use. This new diagnostic system immediately proved its value by allowing us to quickly and precisely adjust the ZnO thickness in the production machine when first using the new reactive sputtering technique developed in Task 7. The machine operators are used to close the loop on this device; eventually we would like to have closed loop control for this device as well as the ITO thickness monitor. A device of this type will be included in the new 25 MW BR machine. We also would like to implement similar devices in the a-Si machine to measure the silicon device thickness.

The PV Capacitive Diagnostic (PVCD) System

In Phase I we bench tested a device and showed that, with a pulsed light source, we can accurately measure the PV voltage vs. time using a non-contacting system. We also showed that we could measure V_{OC}, a quantity proportional to the device short circuit current divided by device capacity, and a fill factor.

This year, in Phase II, we installed a second generation system in the take-up chamber of the 5 MW a-Si production machine and demonstrated that we can easily detect missing layers and track the device V_{oc}. This testing made clear technical issues not obvious on the bench, including the effects of ionized gas, and the need for temperature and position stability. These issues have been addressed in the 3rd generation system that has been designed, fabricated, and is being readied for bench testing. The design (target) stability of this 3rd generation device is 0.1 (0.01)%.

There are some physics issues with respect to this device that are not yet been completely understood, or have not been studied. We have decided that it would be more productive to initially use the 3rd generation system for further bench testing rather than immediately install it in the 5 MW machine.

Task 7: ZnO Reactive Sputtering

United Solar deposits the ZnO layer in its backreflector using magnetron sputtering and ceramic ZnO targets. The manufacturing cost for this layer could be reduced by about an order of magnitude by replacing the ceramic ZnO targets and reactively sputtering the ZnO layer from Zn metal targets. In the Phase I portion of this program we optimized this reactive sputtering process in United Solar's 2 MW pilot backreflector machine. In the Phase II portion of this program we tested and performed initial optimization of this process in United Solar's 5 MW production machine. This backreflector was then processed through the a-Si and ITO roll-to-roll production machines and through QA/QC. The QA/QC analysis showed that the PV material produced with the reactive sputtering process have the same efficiency as cell produced on the standard production backreflector.

In the upcoming few months United Solar will qualify the reactive sputtering process developed in the program and implement it into production. This process will also be used in United Solar's new 25 MW production facility. We estimate that this process will reduce the manufacturing cost by about 0.03$/W.

Task 8: New Deposition Hardware

Although the production machines use the same recipes as our research reactors, the production machines have never been able to produce PV material with the same efficiencies as can consistently be produced in the research reactors. We believe that there are some fundamental differences in between the large area PECVD reactors used for production and the smaller reactors used in research. In addition, there are problems observed with large area reactors that are not observed in small area reactors, such as changes in the uniformity of deposition thickness with deposition rate. This change in deposition thickness uniformity with deposition rate is observed to a large degree in the present large area production cathodes, and severely limits the dynamic range over with parameters can be varied in optimization studies.

In this Task we are developing and testing new cathode and gas distribution concepts for large area cathodes that will more closely reproduce the results obtained in the small area research reactors and that will provide a higher degree of deposition thickness uniformity over a wider range of deposition rates. In the Phase II portion of this program the 2nd and 3rd generations of cathode hardware have been installed and initially tested in the pilot roll-to-roll machine. With both sets of hardware, the goal of ± 5% thickness uniformity across 80% of the cathode areas has been achieved at deposition rates between 2.9 and 4.3 Å/s rates. These rates are 1.5 - 2.2 times the rates used in production. Using the 3rd generation hardware, efficiencies that are 4% greater than those obtained in the production machine have been achieved for a-Si single-junction cells demonstrating an improvement in I-layer quality. Continued optimization of the cathode hardware during Phase III portion of the program should allow for the achievement of the 6% increase in performance goal.

Task 8A: New Pinch Valve Technology

The turnaround time for the a-Si production machine could be reduced by about 1.5 hr if the cool down and heat up procedures could be eliminated. In this program we proposed designing, fabricating and testing a new “pinch valve” technology that would allow the production crews the ability to change rolls of substrate in the take-up and pay-off chambers without needed to cool down, vent, pump down, and re-heat all the process chambers. Since the a-Si machine is presently the rate limiting machine, the resulting increase in throughput for this machine would directly lead to a corresponding throughput increase for the entire production plant.

This portion of the PVMat Program has been extremely successful – the milestone for testing this device in United Solar’s 5 MW production machine, scheduled for early in the Phase III portion of the program, has already been achieved in Phase II. In the Phase III portion of the program we shall concentrate efforts on making the additional machine modifications necessary, and changes to the interlock, pumping, and sequence of operations necessary to implement this device into machine operations. When this is accomplished, we expect a 6% increase in the throughput for the 5 MW plant. These devices are now being used as models to develop new pinch valves for the new United Solar 25 MW production equipment being fabricated by ECD.

TASK 5 – PROCESS CONTROL IMPROVEMENTS: SUBSTRATE HEATING AND TEMPERATURE MONITORING SYSTEMS

Summary

This portion of the PVMat program has been a tremendous success. We have accomplished all goals as originally proposed, ahead of our original schedule:

- We have designed and built a new, improved substrate heater using flat-ribbon-shaped elements.
- We have completed the pilot and production machine installation of the new substrate heaters.
- We have demonstrated precise temperature control while using the new substrate heaters.
- We have demonstrated suitability of the new substrate heaters in the production machine.
- We have, in addition, demonstrated remarkable improvements in cross-web temperature uniformity.
- Finally, these new heaters, besides improving the operation of the present production equipment, are being adapted for use in the new United Solar 25 MW production equipment being designed and fabricated by ECD.

Introduction – Description Of Problem

The multi-section amorphous silicon alloy deposition machine consists of a pay-off chamber section, nine process chamber sections for deposition of the triple (graded) junction, triple bandgap solar cells, and a take-up section. This machine is a continuous roll-to-roll rf plasma-enhanced CVD processing system, in which mixtures of feedstock gases are decomposed at a pressure of approximately 1 torr in a series of plasma chambers. In each chamber, the substrate is maintained at various temperatures of a few hundred °C, and exposed to various gas mixtures.

In the past, the substrate temperature was maintained by exposing the web to the radiation of infrared lamps. As shown in Fig. 1, these lamps, because they run hot, would get coated with deposition along with the substrate.

Fig. 1. Photograph showing the IR lamps coated with deposition material.

The accumulation of deposition material on the IR lamps, in combination with the unavoidable temperature cycles, eventually resulted in severe flaking and in physical stresses large enough to break the lamp quartz envelopes. Even though the deposition takes place on the underside of the substrate, the growing film is not protected from physical damage from the flakes and from the glass debris. Breakage of the quartz IR lamps leads to downtime, and expense.

Proposal Outline

We proposed to replace the quartz heaters in the roll-to-roll deposition machine with low-temperature, long-lasting NiChrome (a Nickel Chrome alloy) resistance heaters. These heaters operate at lower, more stable, temperatures. More importantly, they were thought to require little, if any, maintenance. They further offer considerable freedom in their design. We proposed to design, prototype, test, and retrofit the deposition machines with a new substrate heating system using flat ribbon-shaped elements held in place over the web with ceramic insulators, in a basic “flat sheet” configuration shown in Fig. 2.

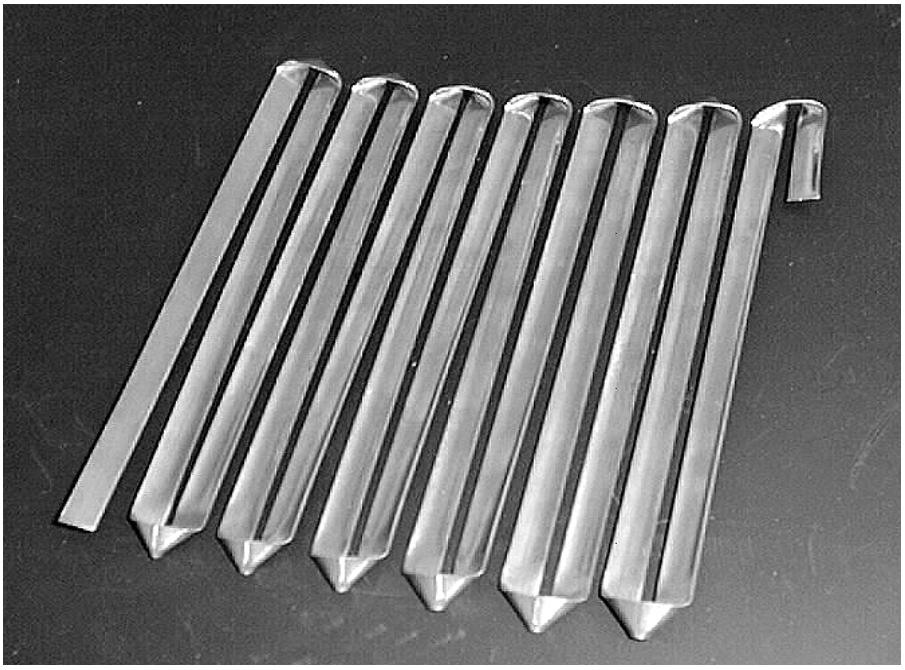

Fig. 2. Photograph of the proposed NiChrome heating element.

These ribbon heaters were initially installed in the pilot machine, using a housing that allowed the shape of the “flat sheet” to be adjusted to a large degree, as shown in Fig. 3. The idea behind the adjustment was to be able to compensate for the generally higher temperatures at the centerline of the web.

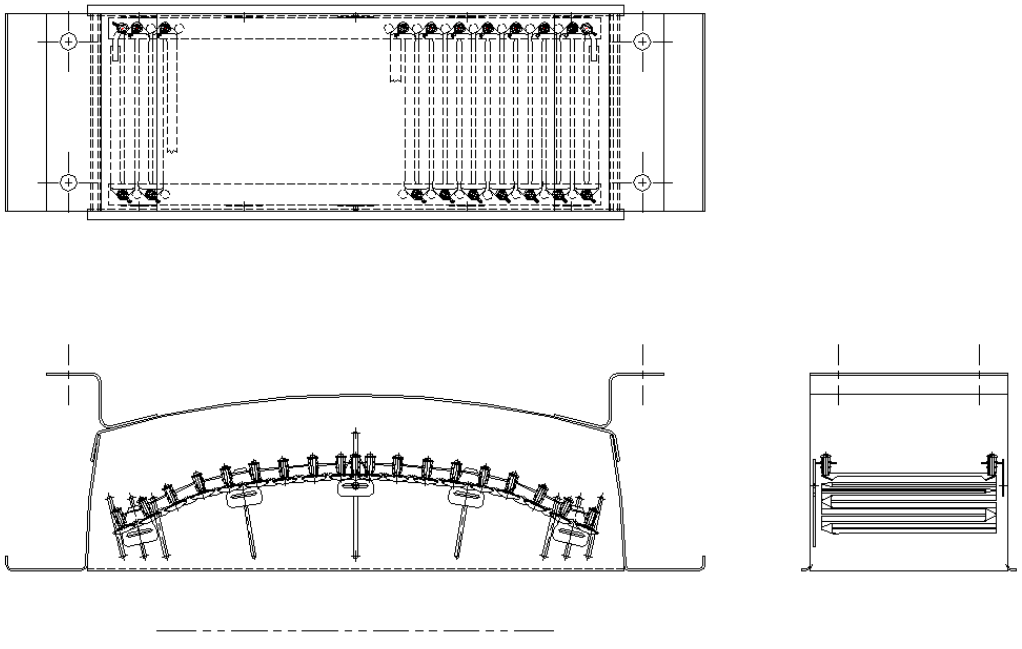

Fig. 3. Sketch of experimental housing

Installation in the Production Equipment

Testing in the pilot machine quickly demonstrated that the reliability of these new ribbon heaters was vastly superior to that of the infrared lamps. Consequently, well ahead of schedule, we decided to fabricate and install ribbon-type heaters in the production machine. Figs. 4 and 5 show their installation.

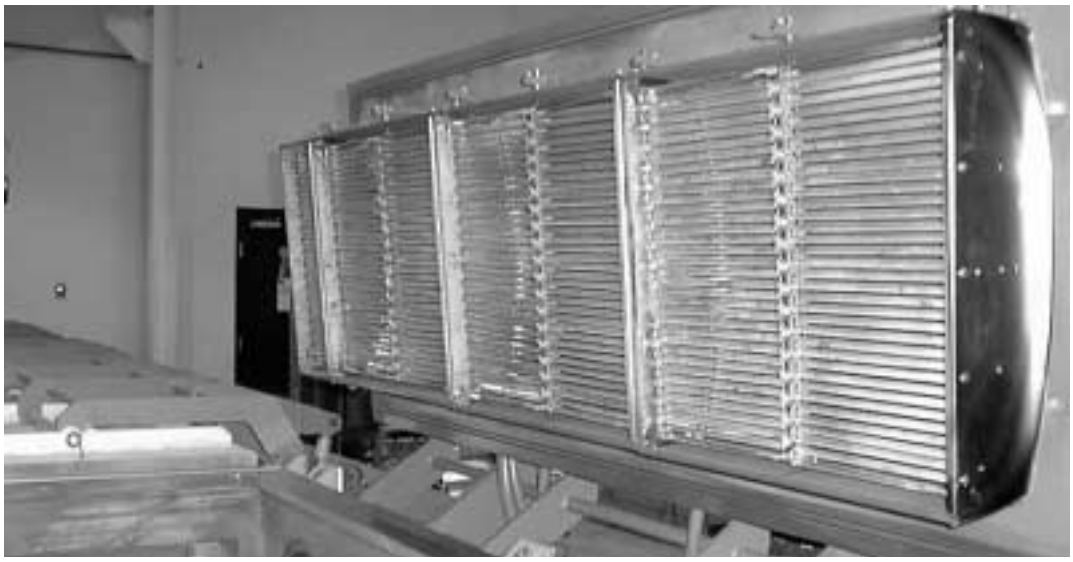

Fig. 4. Ribbon-type heaters installed in the production machine.

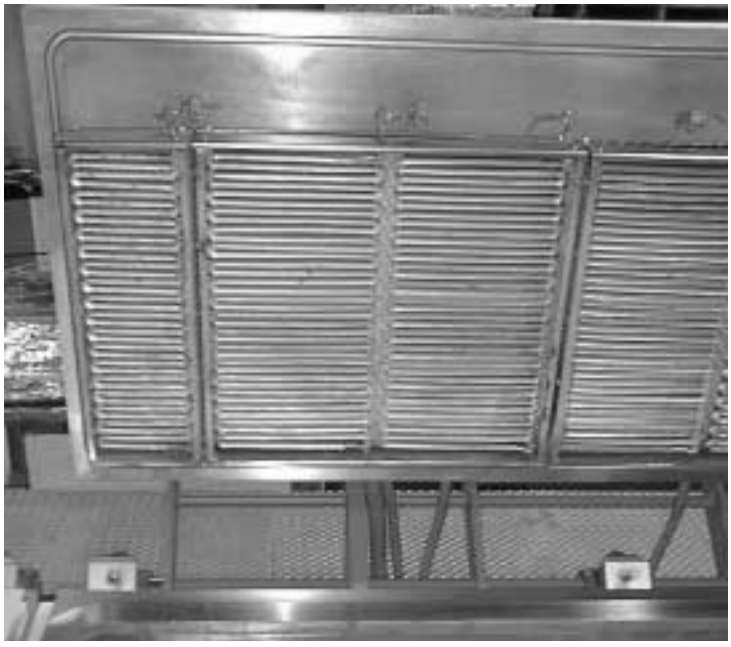

Fig. 5. Ribbon heater assembly detail.

Long Term Operational Experience In The Production Equipment

As of June 25, 1999, the ribbon heaters had contributed to 220 production runs, without any failures no sign of degradation. As of December 20, 1999, the ribbon heaters had contributed to over 300 production runs, with one failure that is described later. In contrast, 120 of the old style infrared lamps would have had to be replaced four times for a similar production quantity, at a total material cost of $40,000.

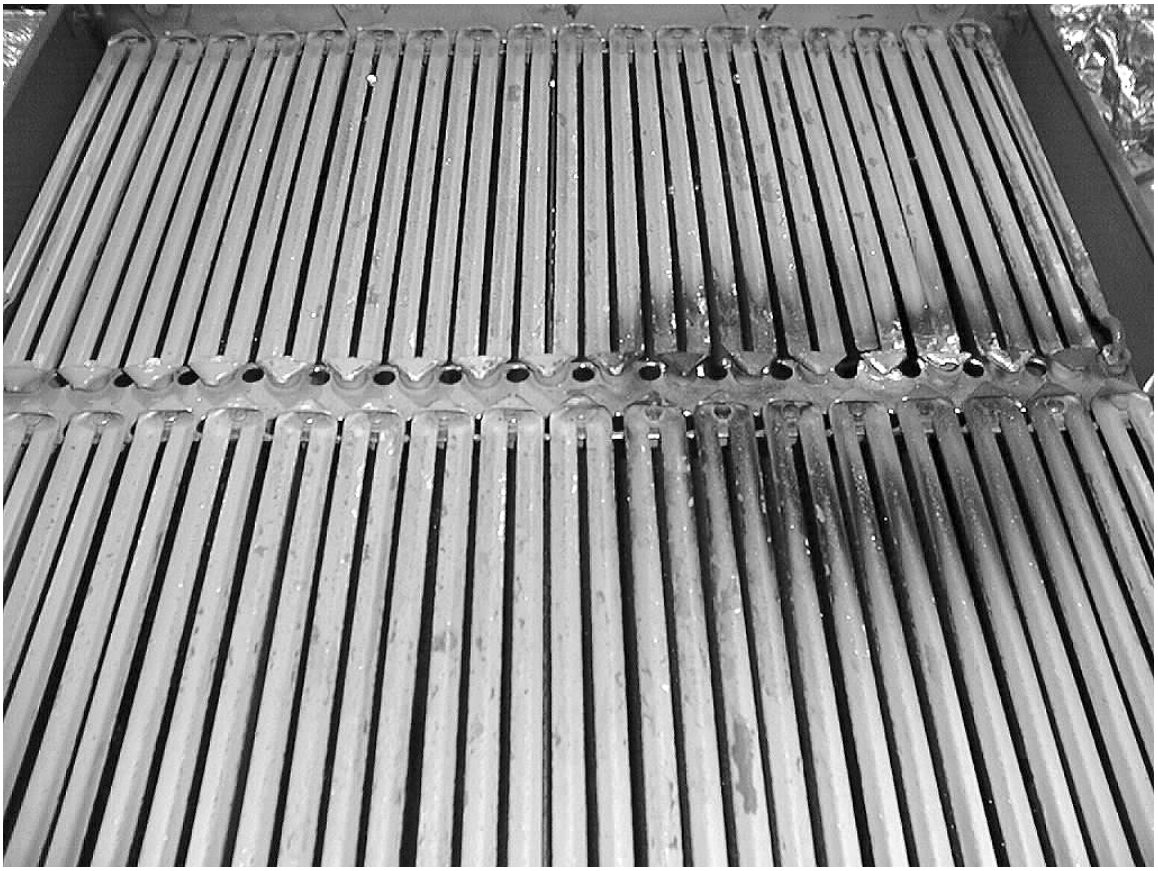

Fig. 6. Photograph of failed heater assembly.

Heater Failure

One of the new ribbon heater assemblies failed in late 1999. A photograph of the failed heater is shown in Fig. 6. A post-mortem analysis has shown that a ceramic isolation post has broken, and that the ribbon had shorted to the grounded chassis. It is not clear, however, whether the failing post caused the ribbon to short, or whether excessive local heat from a defective ribbon element overheated the post. Further analysis has revealed that the heater elements have become brittle, probably due to chemical reactions with the feedstock gases used in the deposition reactor. The ribbon heaters show no other sign of visual, electrical or operational degradation. No process contamination has been observed with these heaters.

Temperature Uniformity

We have recently developed a technique that dramatically increases the cross-web temperature uniformity. Fig. 7 shows the measured cross-web temperature before and after implementation of this new technique.

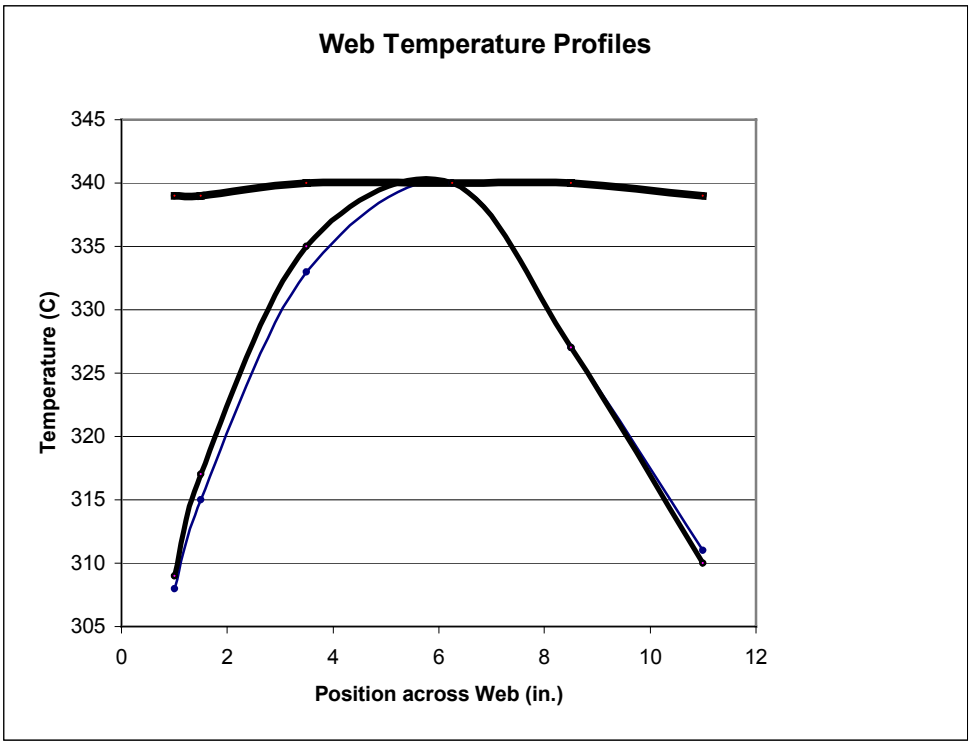

Fig. 7. Web temperature profiles for the various heater configurations. The top thick line shows the temperature uniformity after implementation of the new technique.

TASK 6: DEVELOPMENT OF ONLINE IN-SITU DIAGNOSTIC SYSTEMS

Summary

This portion of the PVMat program (Tasks 2 and 6) has been extremely successful. Three diagnostic systems are currently under development in this program:

1. *BR Reflectometer*. This device measures the thickness of the ZnO films deposited in the roll-to-roll backreflector (BR) machine. This device was installed in the production BR machine ahead of schedule in November 1999 and is now in operation. The reflectometer immediately proved its value by enabling the rapid optimization of reactively sputtered ZnO films in the production machine – Task 7 in this PVMat Program. Further future development work in this area includes:
   - further characterization of the sensor performance (sensitivity, long-term stability);
   - investigation of the correlation between ZnO deposition parameters, reflection data, and cell performance;
   - integration of the system with the present BR production monitor and control system; and finally,
   - development of closed-loop control of ZnO layer thickness and operator interface.
2. *Backreflector Scatterometer*. This device characterizes the texture of the BR material. The second generation device is now being bench tested. This device has evolved considerably in sophistication: the first generation device used for bench testing consisted of a single photo-diode mounted on a moving mechanical arm to measure reflectance as a function of angle. The second generation device contains no moving parts and was designed to be installed in the production BR machine with all electrical components mounted outside the vacuum system. This second generation system uses a fixed laser, a single photo-diode to measure the specular reflectance, and a photodiode array to measure the diffuse reflectance over a wide range of angles.
3. *PV Capacitive Diagnostic*. Much of the effort and resources from the Task 6 portion of this PVMat program have been focussed on the development of this diagnostic system. The first generation system, developed in Phase I, was used for bench testing and demonstrated that this non-contacting device could accurately reproduce cell voltage measurements made with a contacting measurement system. The device demonstrated measurements of V_{OC}, J_{SC}/C, and *FF*. In Phase II we fabricated a second generation device and mounted it in the take-up chamber of the 5 MW a-Si deposition machine where it demonstrated the ability to detect changes in the device quality on-line. Experience with this system enabled us to identify a number of system improvements that were incorporated into the third generation system. This third generation system has been specified, designed, and will be assembled for bench testing in August 2000. The goals of the third generation system are to:
   a) Demonstrate a V_{OC} measurement precision and stability of better than 0.1%. Identify factors limiting precision, stability, and repeatability. Correlate with offline QA/QC data and evaluate.
   b) Demonstrate *FF* measurements. Correlate with offline QA/QC *FF* data and evaluate.

c) Demonstrate J_{SC}/C measurement. Correlate with offline QA/QC J_{SC} data and evaluate.
d) Determine and specify mechanical requirements for 25 MW PVCD system

A summary of the testing in the production machines, and future plans for work on each of these systems follows.

A change from our plans for Phase II was to immediately begin testing these devices in the 5 MW production equipment ahead of schedule rather than testing them in the pilot production machine. The disadvantage of installing the systems in the production machine is that the systems cannot be accessed and modified without affecting production. The advantages of installing them in the production equipment include:

- The production equipment is in daily operation, so the systems can be operated all times. The pilot machines are only operated intermittently.
- The production product goes through a rigorous offline QA/QC, so that we can continuously compare online measurements to off-line QA/QC data.

We have taken the approach of designing the diagnostic systems with all the electronics and detector systems external to the machine vacuum system. This allows us to take advantage of advantages of working on the production equipment without the disadvantage, since the systems can be accessed and modified at anytime without affecting production.

Introduction

United Solar manufactures its PV material using ≈ ½ mile long substrates that are processed sequentially through a series of roll-to-roll deposition machines: the backreflector (BR), amorphous silicon (a-Si), and top conductive oxide (TCO) machines. The QA/QC process takes place after deposition in final roll-to-roll machine, after the long substrate has been slabbed. This is a highly efficient manufacturing process, but can be improved with online diagnostic systems:

1. Online diagnostics will immediately notify operators of any significant problems, consequently reducing the probability that equipment malfunctions or operator errors go unrecognized until the later QA/QC process.
2. The feedback rate for continual optimizing the machines using incremental variations in the standard processing conditions could potentially be increased by several orders of magnitude to less than 1/hr from the present 1/few days.
3. The operators would be able to identify and track fluctuations in process parameters that lead to variations in the quality of cells produced, consequently increasing the material quality.

We already have highly-instrumented and automated production machines with hardware and software feedback systems. These machines are operated open-loop, however, in the sense that sensors monitor process parameters (e.g. temperature, rf power, pressure, etc.) rather than characteristics of the deposited coatings (e.g. V_{OC}, efficiency, I_{SC}, diffusivity of the backreflector, conductance and thickness of the ZnO, etc.). In this PVMat program ECD and United Solar have begun the development and implementation of online, real-time diagnostic systems to measure the characteristics of material produced in the 3 roll-to-roll deposition machines: the backreflector (BR), amorphous silicon (a-Si), and top conductive oxide (TCO) machines. At a minimum these devices have the potential of alerting operators to production problems in a timely fashion; the potential also exists for employing these system for online optimization of material during the production process.

In the first year of this program, hardware systems were developed and tested on the bench, and new second generation systems were designed for installation in the deposition equipment vacuum systems. In the Phase II portion of this program, two of these systems were tested in the production machines in a production environment, and another is completing bench testing prior to installation. Based upon the testing in the production machine, a third generation system for the a-Si machine has been specified, designed and fabricated. We have also begun development of a data base to connect results of online measurements with data from the complete offline QA/QC measurements of the final product.

Backreflector Reflectometer

Status

Fabrication of the BR reflectometer and installation on the United Solar BR deposition machine was completed in November 1999. The system was installed on the United Solar BR production machine rather than the pilot production machine. Mounting the sensor at the gas gate just after the ZnO deposition region enables near real-time monitoring of ZnO layer thickness. Data acquisition software has been developed and the system is currently operating in a continuous monitoring mode, acquiring data every 2 minutes. Data consist of screen plots and computer files containing reflection curves and local reflection minima/maxima wavelengths versus time. The system has been characterized for noise and reproducibility, with sensitivity and long-term stability to be further studied. Reflection data of several standard production and experimental runs have been analyzed. Correlation between reflection data and solar cell performance has been briefly studied.

Further steps in development include:

- further characterization of sensor performance (sensitivity, long-term stability);
- investigating the correlation between ZnO deposition parameters, reflection data, and cell performance;
- integrating the system with the present BR production monitor and control system; and
- developing closed-loop control of ZnO layer thickness and operator interface

Measurement Summary

Standard BR. After bench calibration using a front surface silver mirror as a reference, the system was installed on the BR production machine. Several runs of standard BR deposition were measured in these initial tests. Figure 8 shows a typical reflection curve at one point near the beginning of a run. Typical ZnO layer deposition results in one minimum between 800 - 900 nm and one fairly consistent maximum near 600 nm. The variation of the minimum is not fully understood at present and will be investigated further. It is suspected to be an artifact of the measurement system rather than a real change in ZnO film thickness. The reflection value (BR reflection signal normalized to the silver reference reflection) at the minimum and maximum wavelengths, can vary by as much as 50% from the beginning to the end of a run as seen in Fig. 9. This is believed to be the result of changing aluminum texture, or specularity, rather than ZnO film thickness.

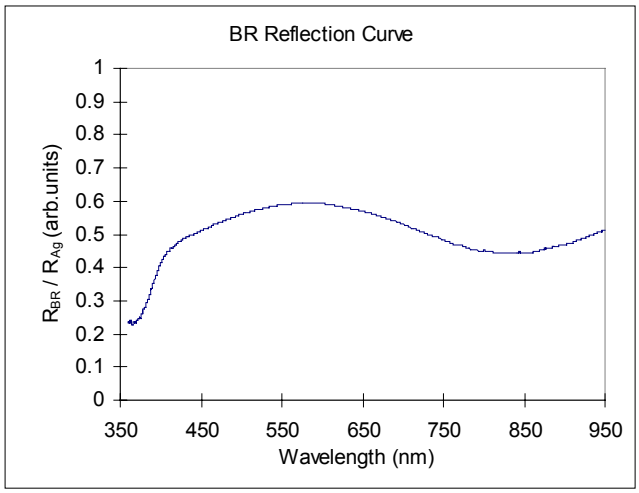

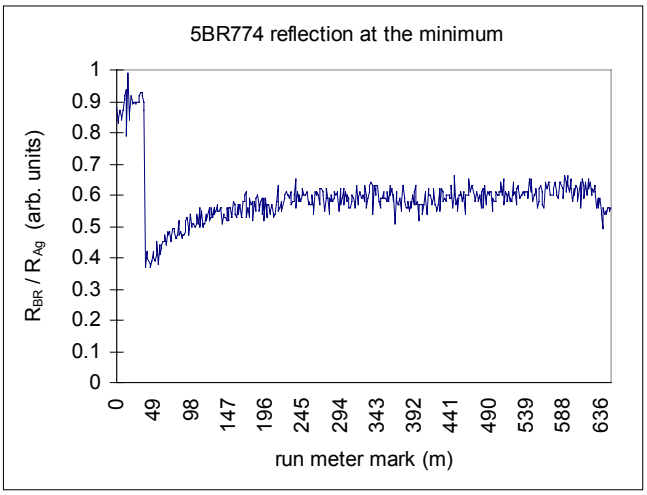

Figs. 8 – 9. Fig. 8 (left): Plot of the BR reflection curve showing the single maximum near 590 nm and single minimum near 810 nm. Fig. 9 (right): Plot of the detected reflection minimum over the course of a complete BR run.

Reproducibility. A 3-5% noise level was observed in these initial BR measurements (Fig. 9). It was discovered that the moving web was the cause of this signal variation. Comparison between static and moving web measurements are shown in Figs. 10 and 11. Each figure plots 5 consecutive scans, taken about 10 s apart. The moving web resulted in a 3-5% variation over the 400-1000 nm range, whereas a static web had 0.5% variation. Since the sensor is positioned at a portion of the web which is between magnetic rollers, it is conjectured that slight web flexing is occurring. The resulting small angular changes in the web surface cause the 3-5% fluctuation in measured signal. Noise pickup due to web drive motors and power supplies were ruled out by dark measurements under static and moving web conditions. Minimizing reflection signal noise level may be achieved by signal averaging.

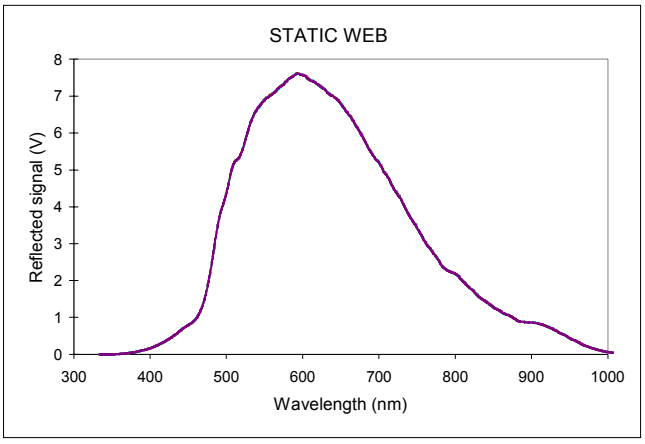

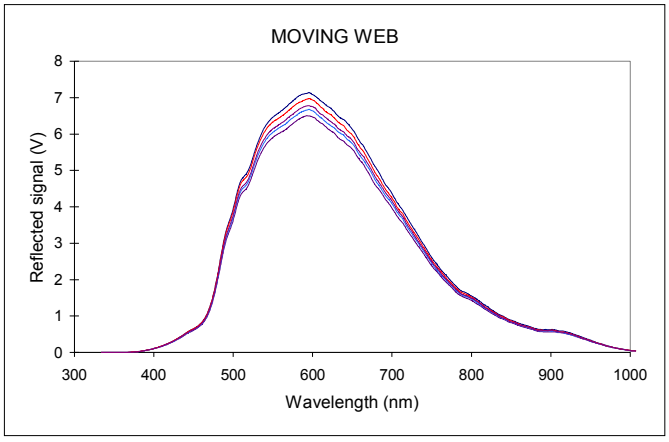

Figs 10 – 11. Five consecutive scans under static (left hand graph) and moving (right hand graph) web conditions.

BR Experiments:

Several BR deposition experiments were performed (some during production runs) to observe the sensitivity of the reflectometer to deposition parameters. In one experiment, sputtering power to one of the six ZnO cathodes was disabled, in effect reducing the ZnO layer thickness by a factor of 1/6. The reflectometer easily detected the resulting decrease in film thickness, as seen by a ~20% shift in the reflection curve minimum as shown in Fig. 12.

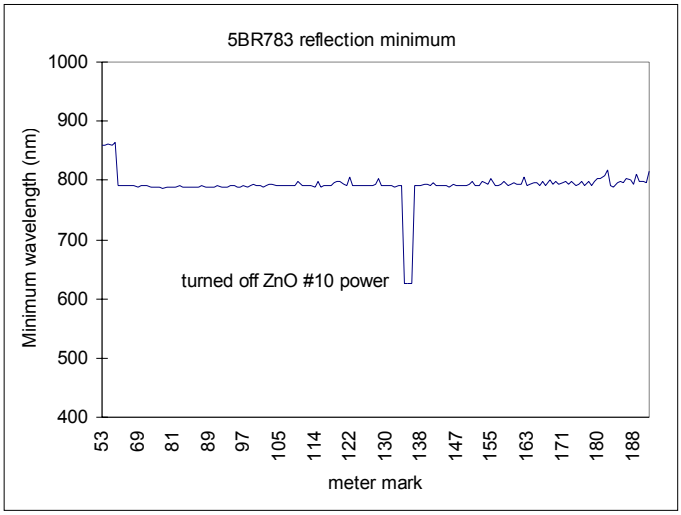

Fig. 12. Plot showing the change in the reflection minimum during the period of time when the ZnO thickness was reduced.

Another experiment varied a deposition parameter, which is referred to here as "x". Several reflection curves taken over a period of 25 minutes are shown in Fig. 13. The reflectometer sensed the effect of the parameter "x" change on the BR deposition during its transition, eventually stabilizing to a 15% decrease in reflection amplitude.

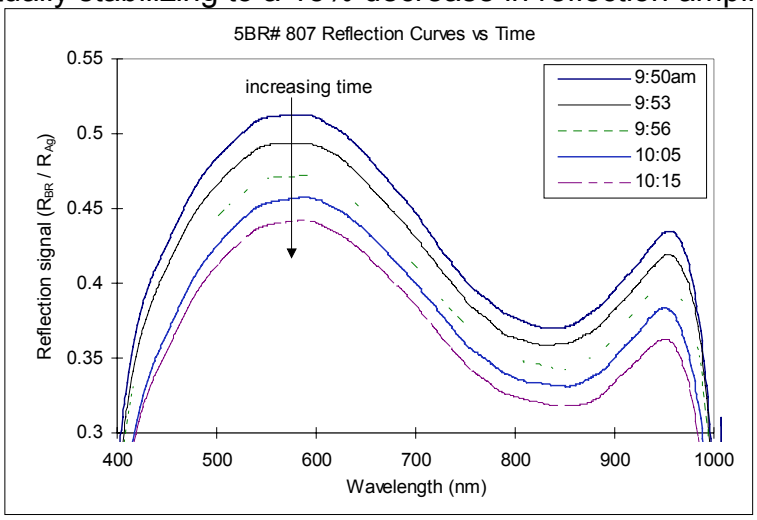

Fig. 13. Plot of 5 reflection curves recorded over a 25 minute period the transition of deposition parameter "x".

A third experiment consisted of reactive-ZnO sputter deposition by which a metal Zn target was used in a reactive oxygen atmosphere (Task 7 in this PVMaT program). The reflectometer was used to determine the equivalent reactive-ZnO sputtering power required to produce typical standard production ZnO layer thickness. The reactive-ZnO sputtering power was adjusted until the reflection curve was similar to that of standard ZnO deposition as shown in Fig. 14. While the minimum and maximum were similar, a 9-12% higher reflection signal is observed for the reactive ZnO film over 450-1000 nm possibly indicating that the reactive-ZnO film is more transparent than the ceramic sputtered film.

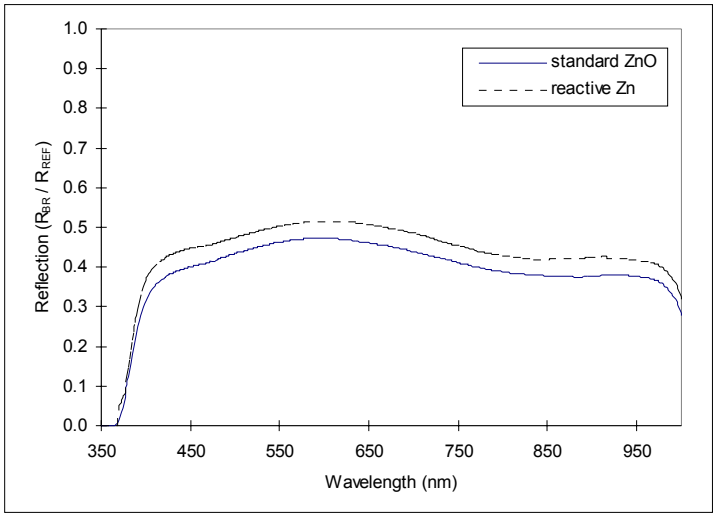

Fig. 14. Plot comparing standard ZnO and reactive ZnO reflection curves.

Reflection Data / Cell Performance Correlation. Reflection measurements were performed off-line on three different types of BR samples. Reflection curves are shown in Fig. 15. Sample 5BR79 is specular aluminum with thick ZnO film, 5BR807 is textured aluminum with thin ZnO film, and 5BR832 is textured silver with thick ZnO. The thicker ZnO films of 5BR79 and 5BR832 are evident by the numerous interference minima and maxima. The specularity of 5BR79 is also evident by its higher reflection signal.

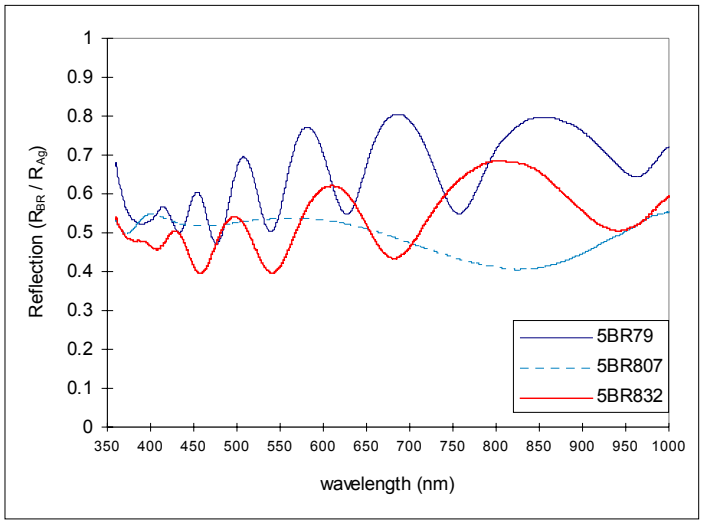

Fig. 15. Plot of various back reflector samples having different ZnO thickness.

The I-V characteristics and quantum efficiency for these samples were measured and are listed in Table I. A 610 nm longpass filter was used for I-V measurements in order to focus on back reflector and bottom cell performance.

Table I: I-V and QE Data for λ>610 nm of R&D Bottom Cells Fabricated on Various Production Back Reflectors

5BR	Type	J_{SC}	V_{OC}	*FF*	P_{MAX}	*QE*
79	specular Al, thick ZnO	10.1	0.591	0.591	3.68	10.22
807	textured Al, thin ZnO	10.8	0.589	0.609	4.07	11.25
832	textured Ag, thick ZnO	11.8	0.591	0.575	4.08	12.02

Comparing the data in Table I, the textured Al-thin ZnO back reflector (5BR807) shows better performance than the older design of 5BR79. The P_{MAX} of the textured Al and textured Ag back reflectors are similar, although the textured Ag has higher J_{SC} and *QE*, and lower *FF*.

Backreflector Scatterometer

Phase II work on this device has included the:

- design and fabrication of the 2nd generation system for the BR production machine (mounting hardware, sensor electronics, etc.)
- bench assembly of the mounting hardware and sensor electronics
- signal interfacing of the photodiode array, driver board, and computer I/O
- software development for photodiode driver control and data acquisition / storage
- initial operation tests and signal optimization

Testing is currently being conducted on the bench under simulated machine port conditions and geometry. Characterization of electrical noise and background signal, and initial measurements of various BR, mirror, and diffuse samples are being performed. Upon completion of bench tests, the sensor will be installed on the United Solar production BR machine rather than a pilot machine. Once installed on the machine, the following will be investigated:

- on-line system stability and reproducibility
- the effect of the moving / flexing web on the diffuse and specular reflection signal
- sensor sensitivity to BR texture
- correlation between BR deposition parameters, reflection data, and cell performance
- integration of the system with the present BR production monitor and control system
- development of operator interface for closed-loop control of BR aluminum texture

PV Capacitive Diagnostic (PVCD) System

This system is designed to measure the PV material V_{OC}, I_{SC}/C, and *FF*. The second generation system hardware was installed in the take-up chamber of the 5 MW production machine in July 1999. The electronics were installed and debugged in August 1999. The system was then operated for several months. Based upon this work, a 3rd generation system was specified, designed and fabricated. It is now being readied for bench testing.

System Debugging

A principal difference between the benchtop system and the 2nd generation system installed in the production machine was the electrical noise environment – while the system tested on the bench had fairly low levels of EMI/RFI, the 2nd generation system had a very high level. The 10^{12} Ω input impedance amplifier is very susceptible to small electric and magnetic fields. There were two principle noise sources:

1. rf from the deposition cathodes. This rf noise was easily filtered, as there is not any signal information at the rf frequency.
2. Line frequency 60 Hz (and homonics) from ground loops and from the pulse width modulated heater circuits. The line frequency noise could not be filtered without distorting the PVCD. To minimize the noise we installed pre-amplifiers on the PVCD high input impedance grid amplifier and the laser photo-diode detector inside the vacuum chamber. These amplifiers boosted the signal amplitude without affecting the 60 Hz noise amplitude, consequently increasing our signal to noise (S/N) ratio. To further reduce the effect of the 60 Hz signal we triggered the PVCD laser asynchronously from the a.c. line frequency and averaged multiple signals on the data acquisition computer. This reduced the effect of the line-frequency interference to a level below far below errors from other effects, such as slow drift due to temperature changes in the web. The system short term drift was on the order of 0.2% peak-peak, as shown in Fig. 16. In the 3rd generation system, which incorporates a web temperature stabilization system and is specified for a precision and accuracy of less than 0.1%, we may have to re-visit this problem. Moving the data acquisition system closer to the sensor and minimizing the distance we need to transport the analog signals can further reduce the noise. Alternately, if we do experience a problem with line frequency interference, we can trigger the system synchronously with the line, and subtract a measured background signal.

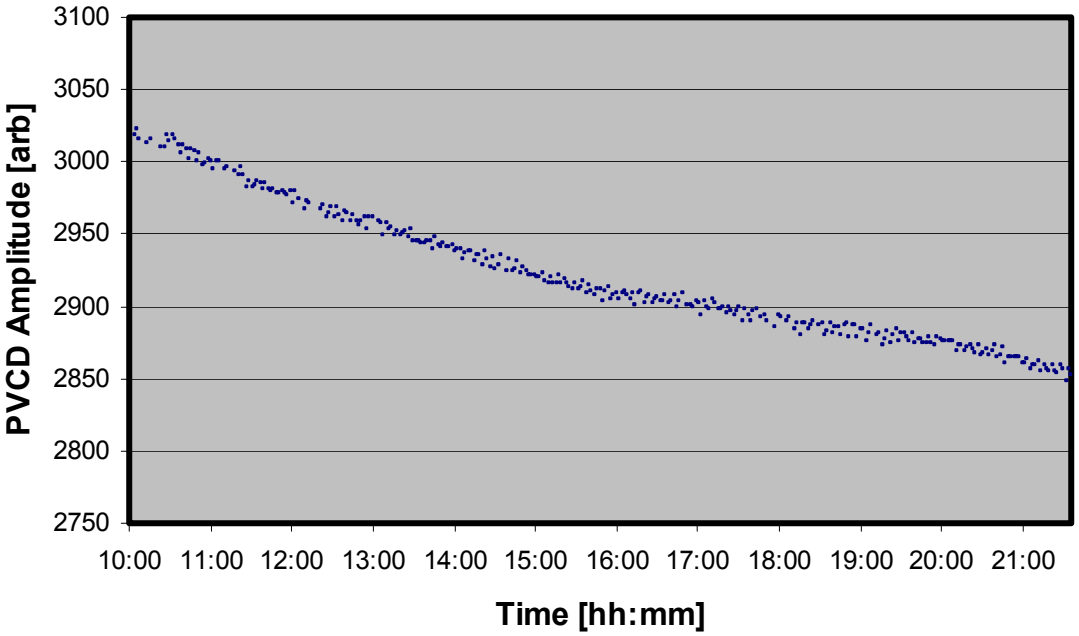

Fig. 16. Graph showing the stability the 2nd generation PVCD V_{OC} measurement (1% full scale/div). Whereas the noise level is on the level of 0.2% peak-peak, there is a 3% drift caused by temperature changes in the web and electronics.

Initial Operation

Signal Amplitude Enhancement. We immediately encountered an unanticipated effect not observed on the bench -- a 6-fold enhancement of the PVCD signal from the sensor grid that occurred when there was a plasma in the P3 chamber upstream of the gas gate which is upstream of the take-up chamber. This enhancement is shown in Figs. 17 - 18. Besides increasing the signal amplitude, this effect also changes the shape of the signal waveform. We observed that:

- The effect was very dependent upon the pressure; a 30% decrease in pressure significantly changes the waveform (significantly increasing the time constant of the enhancement effect).
- The enhanced current was a displacement current: there is no DC current
- High electric field clearing electrodes did not affect this enhancement.
- The effect was very constant and stable.

The effect can be explained as follows (refer to Fig. 19): C_{IN} is about six times larger than C_1 due to the added capacity of the cable connecting the amplifier to the grid, and the input capacitance of the FET amplifier. Consequently, the grid voltage is about 1/6th the voltage of the PV. We conjecture that there is a small amount of ionized gas in the region of the detector when there is a plasma in the P3 chamber. This causes current to flow between the PV surface and the grid electrode (Fig. 19) causing the grid electrode, which is mounted below a sheet of glass, to charge up to the potential of the surface of

the web. When we removed the glass sheet mounted to the sensor grid, we observed a greater enhancement since the current could go directly to the grid, which has a very high input resistance (about 10^{12} Ω).

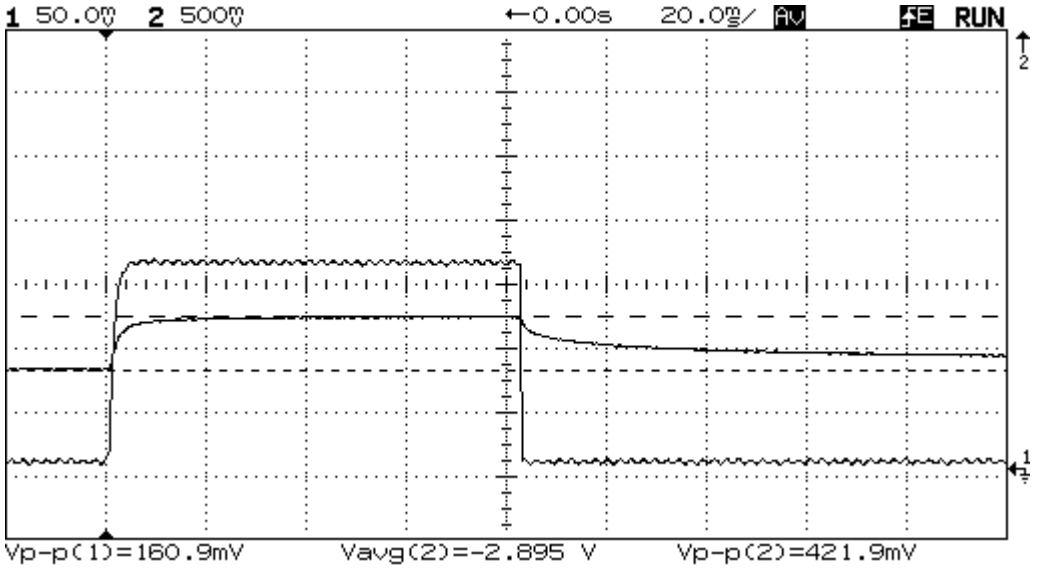

Fig. 17. Waveforms from the laser photodector (trace with the fast turn-off time) and PVCD signal (amplitude 422 mV) when there is no plasma in the P3 chamber.

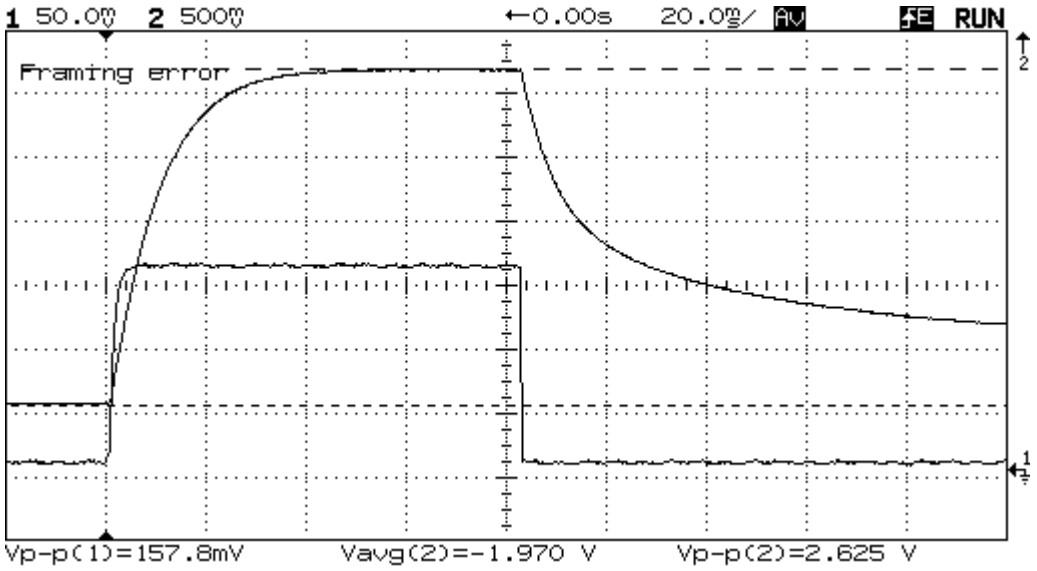

Fig. 18. Waveforms from the laser photodector (trace with the fast turn-off time) and PVCD signal (amplitude 2625 mV) when there is a plasma in the P3 chamber.

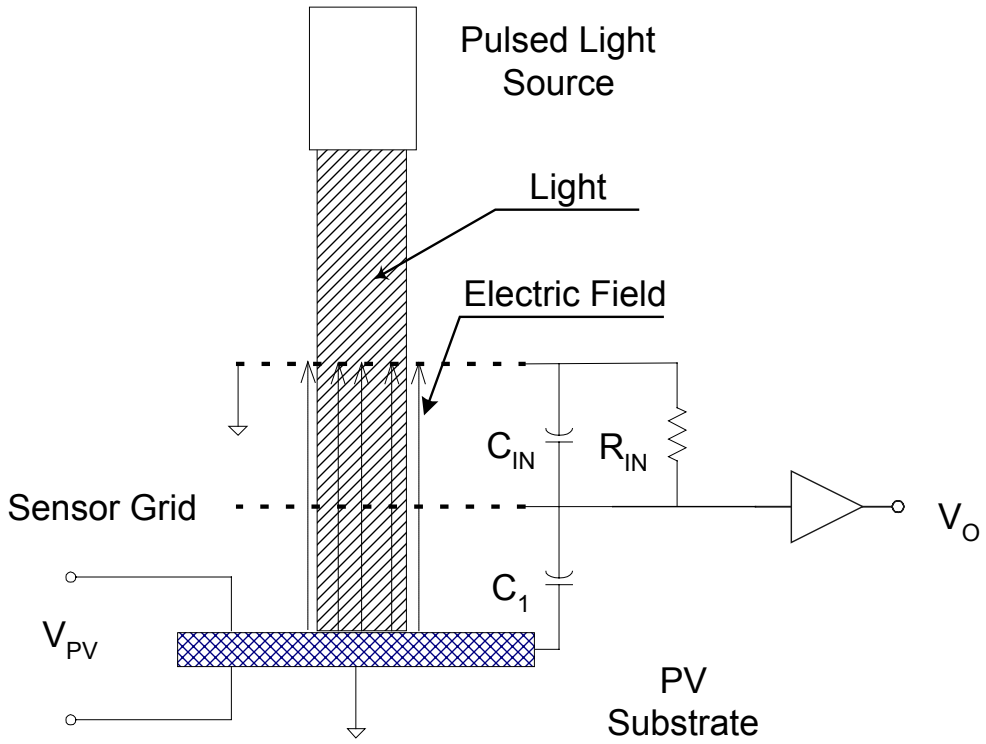

Fig. 19. Conceptual schematic of the PVCD.

Though we have since performed a number of tests showing that we can eliminate this effect, there are still some questions about how to create this effect. Further testing will be performed in Phase III to confirm our understanding.

Initial Stability Testing

Prior to adding the computer data acquisition system in September 1999, the United Solar Systems operator's kept an approximately-hourly log of the PVCD amplitude and laser pulse amplitude and offset. These early results are displayed in Fig. 20.

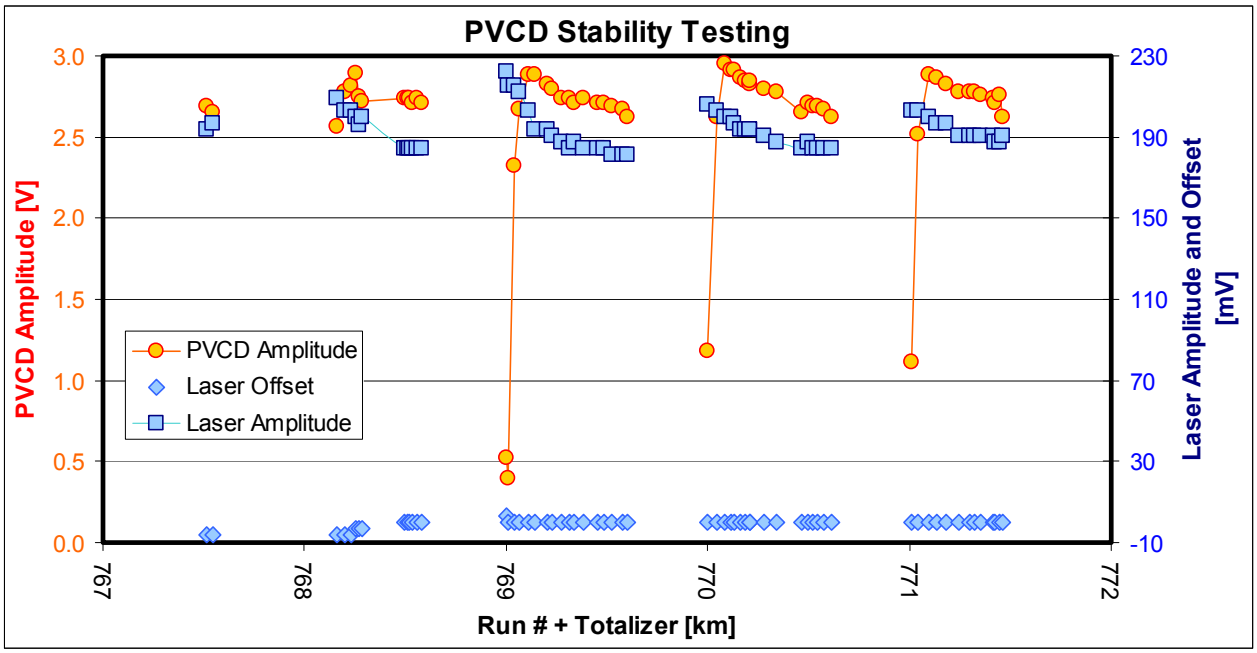

Fig. 20. PVCD signal amplitude and laser pulse amplitude and offset recorded by the 5 W Operations Group.

The most obvious feature in Fig. 20 is the drift in the signal amplitude with time. Since the PVCD drift was correlated to the drift in the laser amplitude, we first mistakenly attributed the PVCD drift to the laser drift. In retrospect we should have realized that the laser drift was not the first order cause of the PVCD drift since the PVCD amplitude varies with the logarithm of the laser intensity. This became obvious after we stabilized the laser amplitude. Rather, both the PVCD and laser drift were a consequence of the changing temperature of the web and electronics in this region, with the web temperature being the first order effect.

One can also observe in Fig. 20 that the last data point in each run tends to be low. This is because this final point is taken at a time when the web has stopped moving. Once the laser has charged up the PV material, it takes 50 – 200 s for the PV material to discharge sufficiently so that the PVCD amplitude is not affected by the previous pulse. We, however, have been operating with a 5 s pulse repetition period, relying on the fact that when the web is moving, every 5 s there is a fresh sample of substrate above the detector.

P3-Layer Tests

We tested the ability of the PVCD device to detect the presence of the top P3 layer. The plasma in the P3 chamber was turned off for a 40 – 50 s period of time, and the output of

the PVCD was monitored. The results are shown in Fig. 21. The six fold enhancement immediately disappeared when the plasma was turned off. About 100 s later, with the plasma back on, one sees a reduction in the PVCD signal amplitude. The signal averaging was not employed during these tests. The PVCD is relatively insensitive to the presence of the top P3 layer with the present low-intensity red (680 nm) laser. Consequently, the ability of the PVCD to detect the absence of this layer, when the averaging was not employed, was very promising.

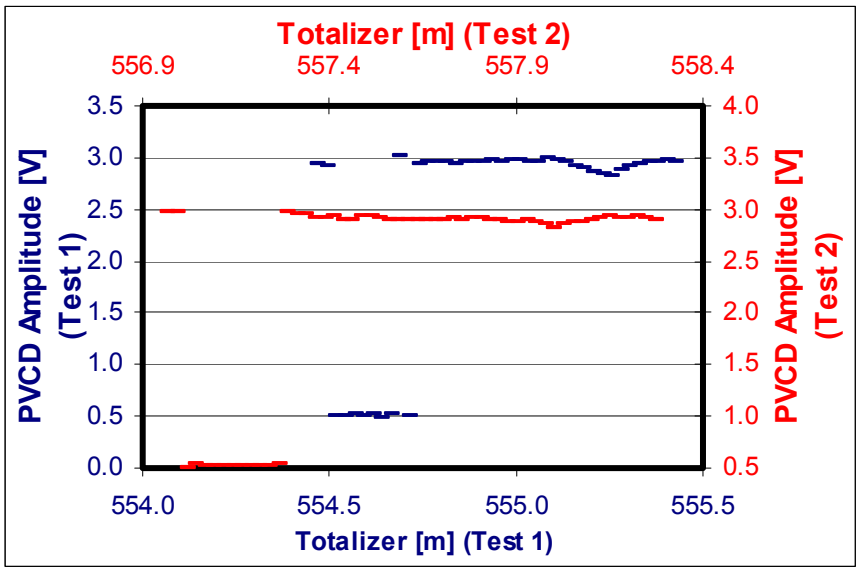

Fig. 21. PVCD signal amplitude measurements taken at 4.67 s intervals immediately prior to and immediately after the P3 plasma being turned off.

Data Acquisition System for the PV Capacitive Diagnostic (PVCD) System

We began by using a digital oscilloscope to the right of the operator's console to display 2 pairs of waveforms from the PVCD as shown in Fig. 22:

1. *Laser Signal* -- The rectangular waveform shown is the signal from a photo-detector and proportional to the intensity of a 30 mW 680 nm laser. When this laser is turned on (at the first vertical graticule line on the scope), the PV material begins to charge up.
2. *PVCD Signal* -- The second pair of waveforms shown is the voltage on the PVCD grid amplifier. The amplitude of this signal, displayed on the bottom of the scope (Vp-p(2)=2.703 V) is proportional to the PV material V_{OC}.

Each signal was displayed twice: a dim waveform showing a reference waveform, and a brighter waveform that was continually updated. If there were a major problem in the 5 MW (i.e., loss of a p-layer), there would be a significant difference between the amplitude of the reference and updated signal.

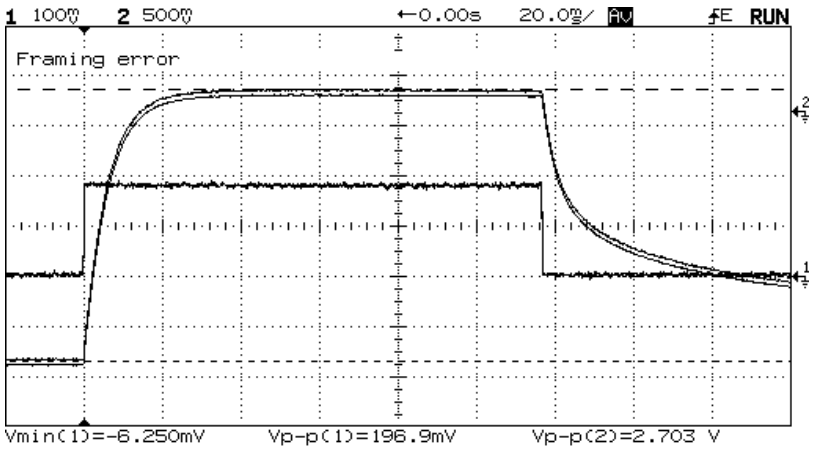

Fig. 22. Oscilloscope PVCD display. (See text).

We were interested in learning about the stability of this device and the operators recorded data on an hourly basis, serving as the data logging system. The data shown in Fig. 20 was recorded in this manner.

In October 1999, we installed a data acquisition and data logging system. The first operator interface was modeled after the oscilloscope display as shown in Fig. 23.

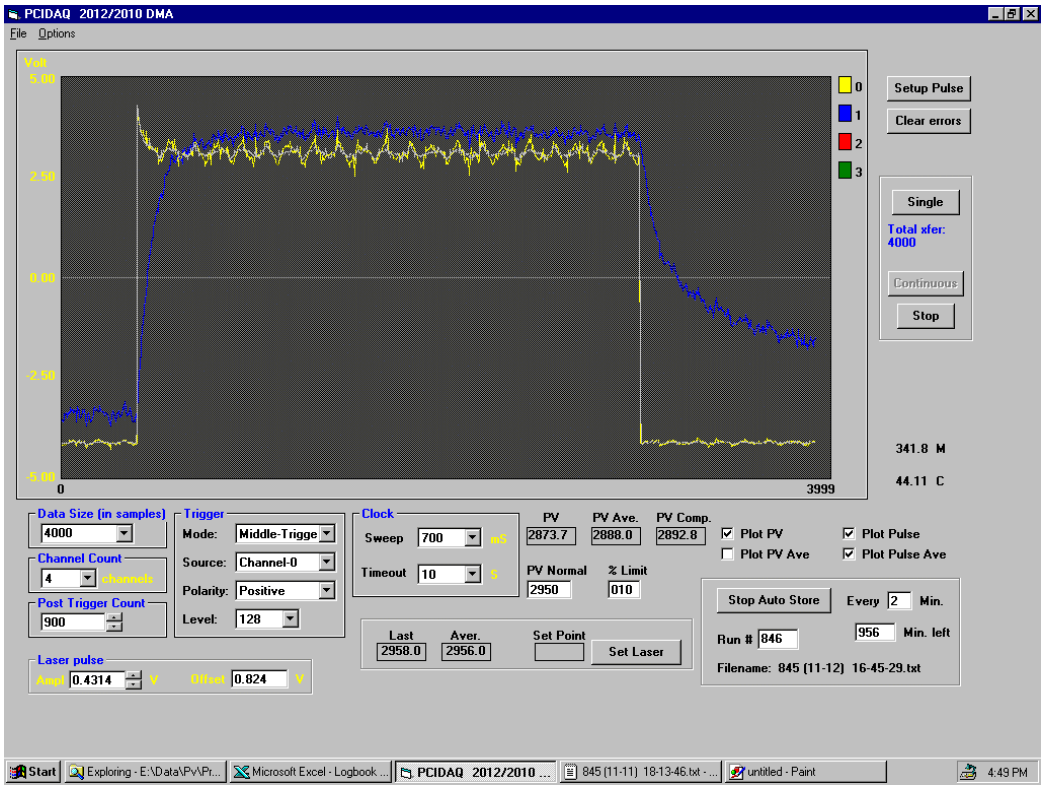

Fig. 23. First PVCD operator interface display. The yellow trace is the waveform of the signal from the photodiode, proportional to the laser output; the blue trace is the PVCD waveform and is proportional to the PV voltage.

The operators were required to type in the new run number at the beginning of each run, and the system logged the measured V_{OC}. If the measured V_{OC} varied by more than 10% from the nominal value, the display background changed from gray to red, consequently notifying the operator that there may be a serious problem in the machine. Due to the large temperature coefficient of the system, primarily due to the change in the temperature of the web, we were not able to put a tighter limit on the V_{OC}.

The display later upgraded to show the measured V_{OC} as a function of time, as shown in Fig. 24. This allowed the operators to immediately ascertain the status of the system, to compare the present run with previous runs, and to observe any sudden changes in the output of the system. As with the previous display, this background changed from gray to red if the PVCD amplitude decreases to a level below the alarm level. This alarm level can be easily changed. We also added a signal from the control computer to the data acquisition system to record the totalizer, or web position.

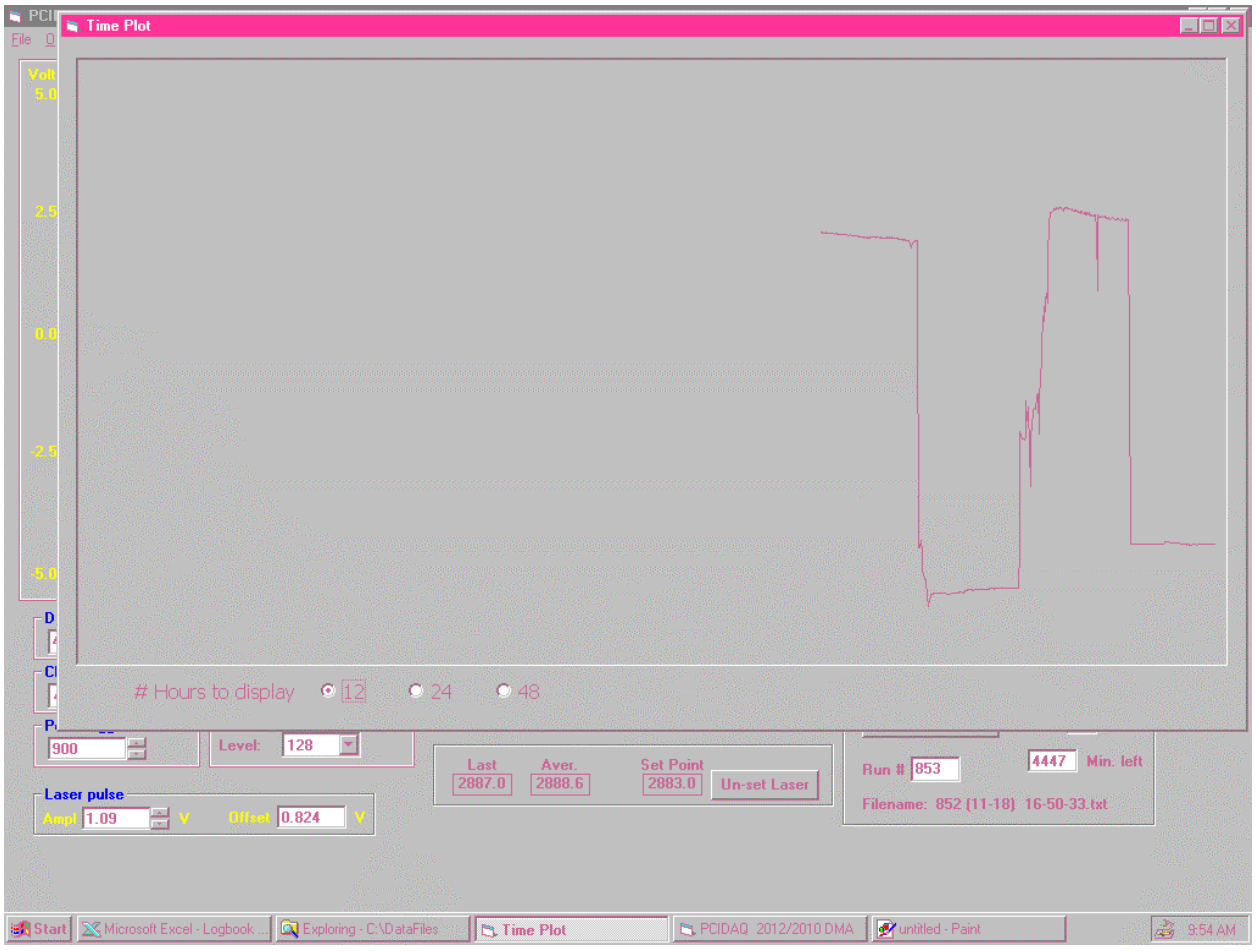

Fig. 24. New PVCD display showing the PVCD amplitude, proportional to VOC, as a function of time.

Comparison with Offline QA/QC

The data acquisition system allowed us to log the amplitude of the PVCD and compare it with offline data. Figure 25 displays a graph of the recorded PVCD amplitude vs. time for about a 2 week period in Nov 99.

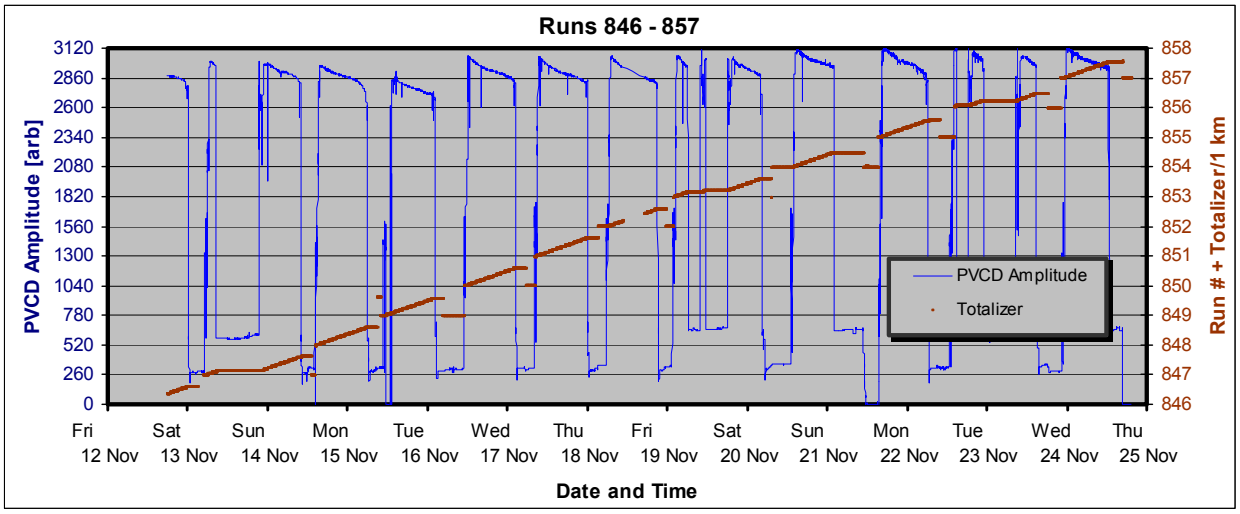

Fig. 25. Recorded amplitude of the PVCD system during a two week period in November. The time periods when the amplitude is low correspond to when the machine is being turned around.

There are a few obvious features of these data:

- The PVCD amplitude slowly and continuously decreases by about 5% during the deposition. This decrease did not correlate with V_{OC} measurements of the product in offline QA/QC
- We also observed changes of about the same magnitude in the over-all level of the PVCD from run-to-run.

We attribute both of these effects to temperature variations on the machine. The web is cooled as it passes through the gas gate between the P3 chamber and the take-up chamber. This cooling, in turn, slowly heats up the mass of the gas gate (by over 10 °C), consequently increasing the temperature of the web we are measuring in the take-up chamber. The PV product has a V_{OC} temperature coefficient of about – 0.38%/°C; the photodiode detector and laser also have temperature coefficients, as does the PVCD itself (via changes in capacities).

In Fig. 26 we show these data corrected modified using a model that assumes a linear temperature coefficient and a thermal time constant of 15 hrs.

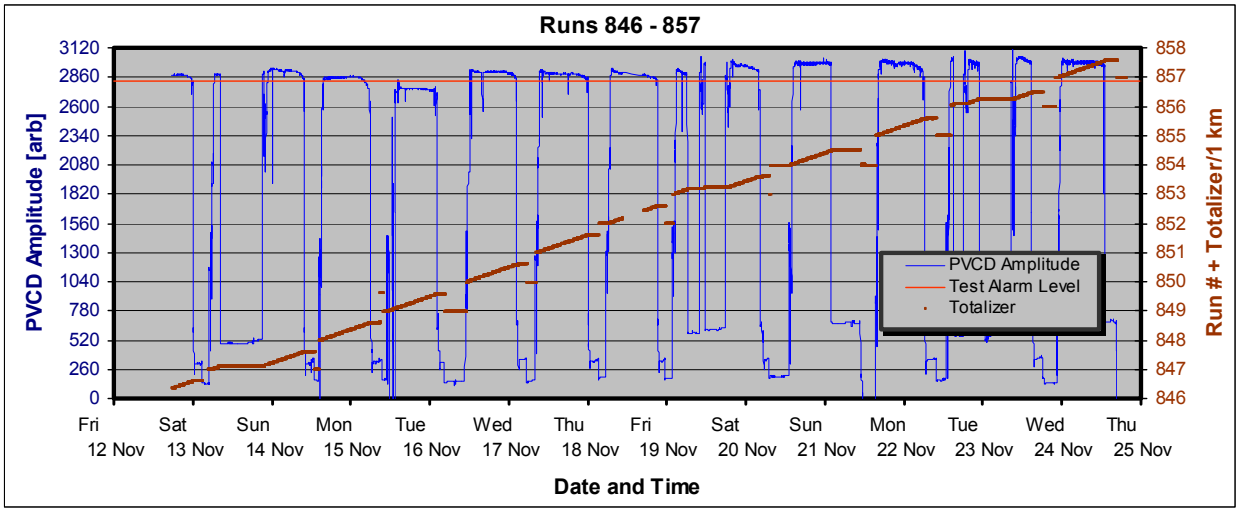

Fig. 26. Data from Fig. 25 re-displayed, corrected using a model that assumes a linear temperature coefficient and a machine thermal time constant of 15 hrs.

These modified data are compared with off-line QA/QC measurements of the V_{OC} in Fig. 27. In these data we can begin to see some correlation between offline QA/QC measurements and the PVCD.

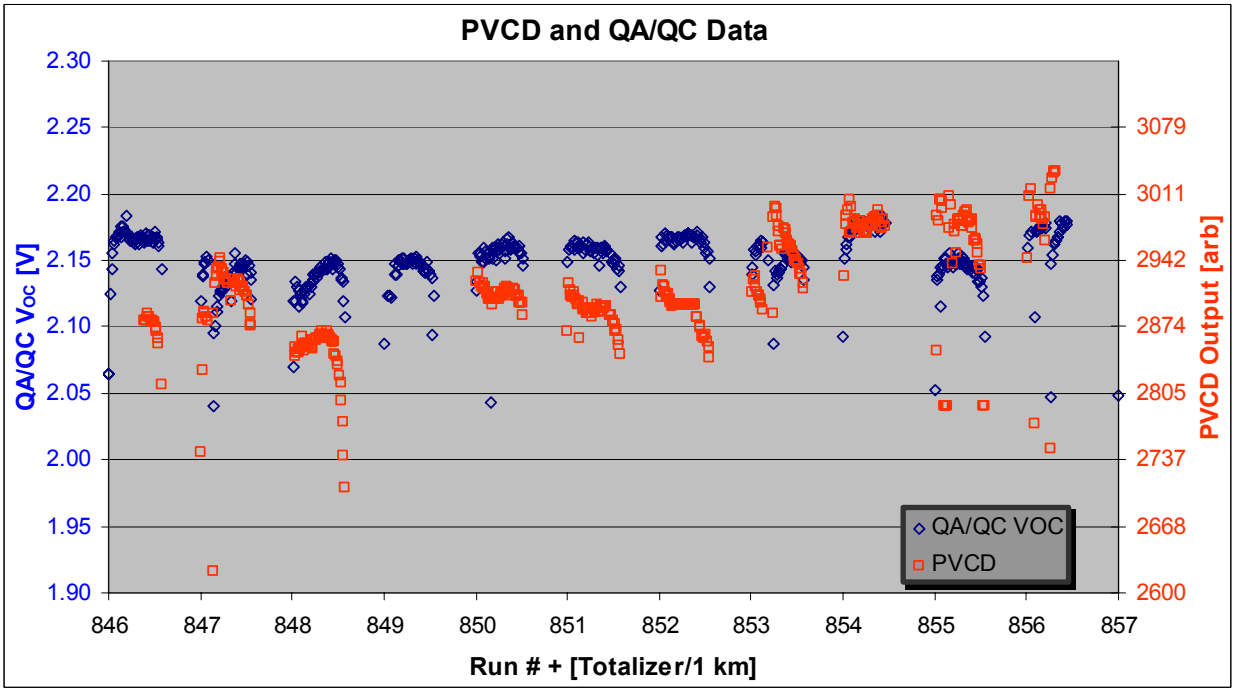

Fig. 27. Online PVCD and off-line QA/QC V_{OC} measurements.

Conclusions from Testing in the Production Machine

Some of the results of our on-line testing, and their impact on the 3rd generation system design are listed below:

- Work in optimizing the system was hampered by the fact that the system could be accessed for modifications only for a short period of time (typically less than ½ hour) between manufacturing runs when the web is changed. Furthermore, this access time may occur at anytime of the day or night. Consequently, 10 minute test that includes 3 iterations for optimization, might involve a week's elapsed time. The third generation system under development has all the electronics mounted external to the machine vacuum system.
- The large temperature coefficient of the PV material, and the large temperature variations of the web and electronics prevented accurate measurements of the V_{OC}. The third generation system being developed includes systems for temperature stabilization of both the web and the PVCD electronics.
- We were limited to measuring only the V_{OC} of the material due to the "enhancement effect" described above. This effect will not be present in the 3rd generation system.
- The third generation system will also use a new white LED light source that will have a higher degree of reliability, more than an order of magnitude more power. The blue light will also enhance the sensitivity to the top layers.

Third Generation PVCD System Design and Plans for Phase III

The 3rd generation system has been designed with the minimum (target) specification of 0.1 (0.01%) stability. A greater precision will allow finer tuning using smaller deviation of process parameters from their quiescent set points. With this system we intend to demonstrate a precision, stability, and repeatability of less than 0.1%. A rendering of this 3rd generation system that is now being readied for bench testing is shown in Fig. 28.

We have decided to first spend a period of time bench testing the 3rd generation device on the bench before installing it in the 5 MW machine. This will allow us to study its response to a range of PV device parameters that could not be observed in the production machine, and consequently, better understand its performance.

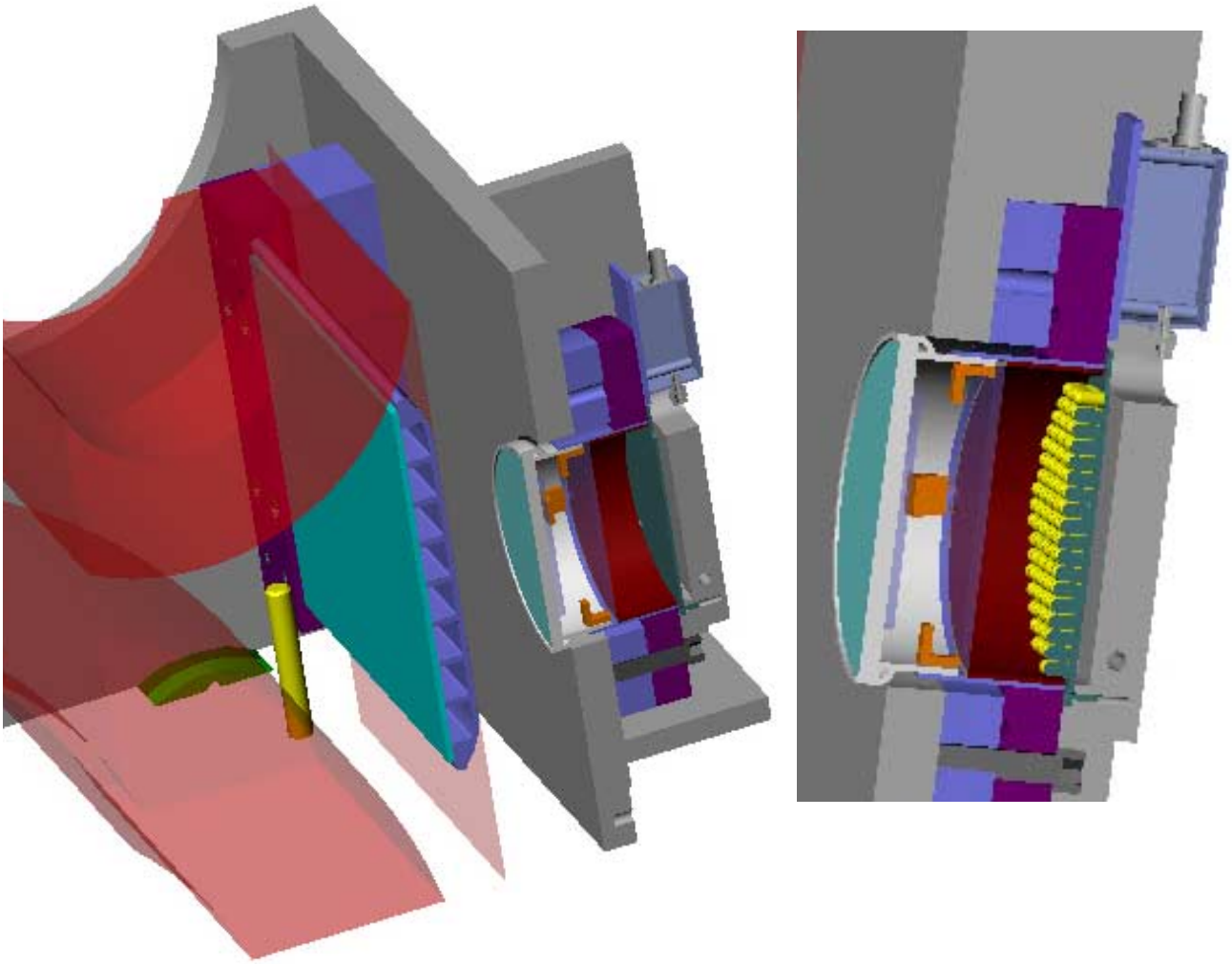

Fig. 28. Rendering of the 3rd generation PVCD.

TASK 7 – DEVELOPMENT OF REACTIVE SPUTTERING PROCESS USING INEXPENSIVE Zn METAL TARGETS FOR BACK REFLECTOR PREPARATION

Background

An integral part of ECD's triple-junction solar cell design is the textured metal/ZnO back reflector that enhances the probability for multiple light passes through the semiconductor absorbing material. The increased number of passes increases the chance for light absorption which in turn leads to higher short circuit currents and higher cell efficiencies. While the back reflectors are needed in order to achieve certain efficiency goals, the cost of making these materials on the production level is significant comparable to that for the semiconductor layer deposition process.

The most significant expense in the magnetron sputtering process used to make the back reflectors is the cost of the ZnO targets. Consequently, if the ZnO targets could be eliminated from the process with a less expensive target, a significant cost savings would result. Since the price of Zn metal targets are $1/5^{th}$ the price of ZnO targets, and conceivably could be made in-house at an even lower cost, reduced cost was a major incentive to test the feasibility of the reactive sputtering process in this program. However, there were other motivations. With the present process, high quality back reflectors are obtainable at production level web speeds. However, at slower speeds (2/3 of the production level speed) back reflectors of even a higher quality can be obtained due to thicker ZnO layers obtainable at these slower speeds. Thus if higher sputtering rates could be obtained, the thick ZnO layers and higher quality back reflectors could be obtained at production level speeds. Since higher deposition rates are likely obtainable with the Zn metal target, improved efficiencies as well as reduced costs might be had with this new process.

Objective of Backreflector Studies

In this program, we are testing the feasibility of using this reactive sputtering process in a roll-to-roll process to verify that it can indeed be used to make long rolls of back reflector coated stainless steel webs in production. In Phase I of the program, a pilot roll-to-roll machine was used to initially test the reactive sputtering process in a moving web environment. This roll-to-roll machine is part of United Solar's decommissioned 2 MW plant and is designed to deposit BR material over a 14 in wide web. To optimize the backreflector deposition conditions, the pilot machine was used to deposit thick ZnO layers onto a stainless steel web previously coated with a standard Al layer and a thin ZnO layer using the 5MW production equipment. To optimize the ZnO layer, a number of deposition parameters were systematically varied including the substrate temperature, the oxygen and argon flows, web speed and power. Also films were made using an Al doped Zn metal target and compared to those made using an undoped target. As a reference, ZnO layers were also made using the standard ZnO targets and the pilot machine.

To test the quality of the back reflectors, a-SiGe:H nip structures were deposited on 2" x 2" experimental back reflector coated substrates using the 13.56 MHz PECVD technique and an R&D deposition system. This system has been used to prepare 1 ft^2

modules with world record efficiencies (>10% stable efficiencies). For each PECVD deposition, nip structures could be deposited on nine different back reflectors. In many of these depositions, high quality back reflectors with the thick ZnO layers made in United Solar's small scale R&D RADLAS system were included for comparison. The back reflectors for most of their world record solar cells and modules were made using this system. The nip structures were then coated with separate 0.25 cm^2 ITO layers for collection. The top contact was completed by depositing Al grids on top of the ITO layers.

In Table II, data for larger area (44.5 cm^2) single-junction a-SiGe:H cells made using the described method. The two cells only differ in the process used to prepare the ZnO layers of the back reflectors. In one case, the standard sputtering process was used while in the second the test reactive sputtering processes was used for fabrication. As can be seen from the data in the table, the properties for the two cells are identical, within experimental error. Thus in Phase I, it was demonstrated that the reactive sputtering process using the inexpensive ZnAl(5%) targets can be used to prepare high quality back reflector material, similar to the material prepared by the standard sputtering process.

Table II. Data for 44.5 cm^2 Modules Made with Different Backreflectors. Measurements made using AM1.5 light.

Target Material	ZnO Deposition Process	BR Machine	J_{sc}(QE) (mA/cm^2)	V_{oc} (V)	FF	R_s (Ω/cm^2)	Efficiency (%)
ZnAl(5%)	Reactive Sputtering	2 MW Pilot	18.9	0.77	0.631	0.20	9.18
ZnO	Standard Sputtering	5MW Production	18.5	0.77	0.649	0.18	9.24

In Phase II, the program goals were:

1) implement the reactive sputtering process into the 5MW production line;
2) demonstrate that high quality back reflectors can be made using the reactive sputtering process and the 5MW production equipment to prepare all the thin film layers; and
3) demonstrate that the high quality back reflector material made consistently over a 100m length using the reactive sputtering process to prove that the process can be reproducibly used over a long production level length.

Experimental

To initially optimize the deposition conditions for the reactive sputtering process in the 5 MW back reflector line, a web was coated with several experimental back reflectors prepared under a variety of conditions. To test the quality of the back reflectors, a-SiGe:H nip structures were deposited on 2" x 2" experimental back reflector coated substrates cut from the web. The semiconductor layers were made using the 13.56 MHz PECVD technique and an R&D deposition system. This system has been used to prepare 1 sq. ft. modules with world record efficiencies (>10% stable efficiencies) and was used in Phase I to prepare the cells whose data is listed in Table I. For each

PECVD deposition, nip structures could be deposited on nine different back reflectors. In many of these depositions, high quality back reflectors with the 5MW equipment and the standard sputtering technique (ceramic ZnO targets) were included for comparison. The nip structures were then coated with separate 0.25 cm^2 ITO layers for collection. The top contact was completed by depositing Al grids on top of the ITO layers.

After initial optimization of the reactive sputtering fabrication conditions, QA/QC coupons were made using the reactive sputtering process to prepare the ZnO layers. For these coupons, all of the layers (back reflector, semiconductor, top contact) were made using the 5MW production equipment. Triple-junction cells were deposited on each of the test back reflector layers. Each coupon contained fourteen 9.7 cm^2 cells for judging the device quality over the entire coupon area.

Cells were characterized using standard IV tests and quantum efficiency measurements. The IV measurements for the a-SiGe:H cells were made using AM1.5 light or AM1.5 light filtered using a 610nm low bandpass filter. The filter simulates absorption due to the top and middle cells allowing only red light which reaches the bottom cell in the triple-junction structure. It is important to compare data obtained using the filter due to the fact that in the high efficiency triple-junction structure, the bottom cell current is the parameter most effected by the use of the back reflector. Also using the filter eliminates any fluctuations in the blue/green light collection which is affected by a number of conditions unrelated to the back reflector including the quality of the p-layer and the ITO layer. The triple-junction cells on the QA/QC coupons were characterized using only the unfiltered light.

Results from 5MW Experiments

In Table III, average data for cells made using the standard 5MW back reflector presently used in production is compared to average data for cells made using the reactive sputtering process. These 0.25 cm^2 cells were prepared using the R&D machines to prepare the semiconductor and top contact layers. The data in the table was obtained using AM1.5 light filtered with a 630nm cutoff filter which only allows red light with wavelengths greater than 630nm to reach the cells. Use of the reactive sputtering process has led to the fabrication of cells with significantly higher short circuit currents but slightly lower open circuit voltages and fill factors. This combination of properties led to cells with similar efficiencies to those prepared using the standard back reflector. These results demonstrated that the reactive sputtering process could be used in the 5MW back reflector production line to prepare high quality back reflectors and bottom cells.

Table III.

Back Reflector Type	Pmax (mW/cm^2)	J_{sc} (QE) (mA/cm^2)	V_{oc} (V)	FF	Rs (ohm cm^2)
Zn Metal - Reactive Sputtering	3.5	10.0	0.58	0.60	11.5
Standard ZnO Sputtering	3.5	9.3	0.59	0.63	11.0

Using the same thin film fabrication process, two 40 cm^2 cells were made, one with the new reactive sputtering process and the other with the standard process using ZnO with

the cell properties shown in Table IV. The cell efficiencies for the cells made using the two back reflectors are similar, achieving the milestone m-2.3.3. These cells were sent to NREL fulfilling the deliverable D-2.3.3.

Table IV.

45cm^2 Modules PVMAT Deliverables for Reactive Sputtered ZnO (5-15-00)

ZnO	Serial #	Area (cm^2)	Temp. (^0C)	V_{oc} (V)	I_{sc} (A)	FF	P_{max} (W)	V_{mp} (V)	R_s (Ω)	R_{sh} (Ω)	Eff. (%)
Sputt. ZnO	7222E1	44.8	21.2	0.641	0.951	0.615	0.375	0.480	0.15	8.3	8.4
	7222F2	44.8	21.2	0.647	0.951	0.620	0.381	0.469	0.15	6.7	8.5
Average		**44.8**	**21.2**	**0.644**	**0.951**	**0.617**	**0.378**	**0.475**	**0.15**	**7.5**	**8.4**
Sputt. Zn	7226E3	44.8	21.7	0.647	0.968	0.610	0.382	0.479	0.15	6.9	8.5
	7226G2	44.8	21.2	0.641	0.968	0.614	0.381	0.476	0.14	7.9	8.5
Average		**44.8**	**21.5**	**0.644**	**0.968**	**0.612**	**0.381**	**0.477**	**0.15**	**7.4**	**8.5**

As previously mentioned, cells were also made using the new reactive sputtering process and the 5MW equipment in ALL of the fabrication steps. That is, the back reflector, semiconductor and ITO top contact layers were all prepared using the 5MW line as is done for the modules to be sold. On the same roll of stainless steel, cells were made using the standard 5MW back reflector fabrication process and using the new reactive sputtering method for final comparison. From this roll, QA/QC coupons standardly used for qualifying the production material were fabricated. Listed in Table V are the average cell properties (14 cells per coupon) for two coupons made using the standard back reflector fabrication process and those for two coupons made using the new reactive sputtering process. One can see that the cell properties are independent of the sputtering process used. The coupons whose data are listed in the table were sent to NREL as the deliverable D-2.4.6.

Table V

Coupon	ZnO Sputtering Process	J_{sc} (mA/cm^2)	V_{oc} (V)	FF	R_s (Ohm-cm^2)	P_{max} (mW/cm^2)
1200	Reactive	6.86	2.13	0.672	37.2	9.81
1275	Reactive	6.91	2.13	0.670	37.1	9.85
1575	Standard	6.85	2.13	0.673	36.1	9.80
1625	Standard	6.84	2.13	0.675	36.0	9.82

We are now in the process of writing a report describing the hardware changes to the production machine for the implementation of the reactive sputtering process. This will be the last deliverable for this part of the program (D-2.4.7) and will mark the end of this section of the PVMaT program concerning the reactive sputtering process. All of goals set for this section of the program were met.

TASK 8 - CATHODE HARDWARE STUDIES FOR A-SI(GE):H I-LAYER DEPOSITIONS

Background

Efficiencies for small area a-Si:H based devices are being steadily increased; the present world record is 13% stable efficiency for a small area triple-junction cell (0.25 cm^2 active area) produced in a small scale reactor (4" x 4" maximum deposition area) by United Solar. This accelerating improvement suggests that even higher efficiencies should be obtainable. However, the efficiencies obtained for large area solar modules are still significantly lower than the 13% values being near 8-9%. The lower module efficiencies are due in part to back end processes such as lamination and module designs. However, even the small area cells fabricated in the large area, continuous roll-to-roll machines (in particular the 5 MW machine) have yet to demonstrate efficiencies that match the world record values even though thorough optimization studies have been carried out. This suggests that there are inherent problems with the present large area process and/or hardware designs that limit the efficiencies to their present day values.

One problem which is more difficult to achieve in the present large area production machines as compared with the smaller R&D machines is the ability to prepare reasonably uniform film depositions across the entire cathode area during PECVD depositions. This problem was of major concern during our optimization program for the 5 MW production machine. For example, a-SiGe:H i-layer depositions, in order to obtain relatively uniform film depositions across the length of the cathodes for each vacuum chamber, we were limited to work in a small area of deposition parameter space. If parameters outside this space were used, gradients across the length of the cathode were obtained for the Ge content as well as for the deposition rate as is shown in Figure 29. It was found that these non-uniformities were <u>not</u> related to unequal power distributions across the cathode or gas depletion, as one might expect. With a moving web substrate, this effect lead to cells and modules which had significant variations in the Ge content through the depth profile of the a-SiGe:H i-layers. Variations in the bandgap of the materials obviously accompanied the Ge content fluctuations that likely formed shallow carrier traps in the i-layers limiting the carrier collection and cell efficiencies. Also, since the quality of a-Si:H based materials prepared by the PECVD method depend strongly on the film deposition rates, the variations in the deposition rates led to the formation of high quality material in the region of the cathode where the deposition rates were low and poorer quality material in the region where the deposition rates were high. Under these conditions, the overall film and device performance was limited by the poor material produced in the high deposition rate region. If the overall deposition rate were lowered in order to improve the material produced in the high deposition rate region, the machine throughput was unacceptably low.

We should note that similar variations in the deposition rates across the lengths of the cathode were also observed for a-Si:H layers. Thus the non-uniformity problem was not related to differences in the decomposition rates of Si and Ge source gases but instead is inherent to the existing vacuum hardware design.

When limited to a small region of parameter space, the efficiencies are likely limited to low values. With a different internal hardware design that allows for uniform depositions across a large area of parameter space, the maximum efficiency would likely be outside the small area of parameter space we are presently restricted to. Thus, if such a deposition hardware design could be devised, higher cell and module efficiencies would likely be obtained.

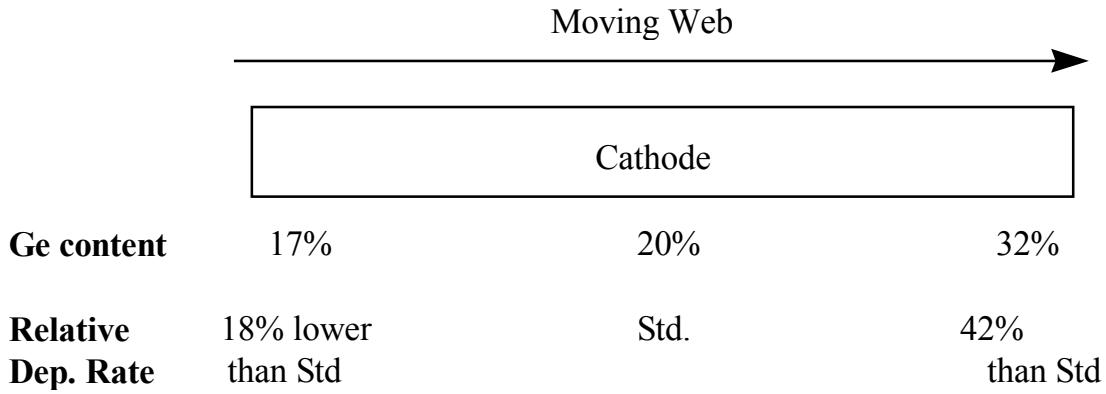

Fig. 29. Variation of Ge content and deposition rate across cathode.

In attempting to achieve the record high efficiencies using the large machines, one must be assured that the film growth conditions used to prepare the large modules are similar to those obtained using the small area machines. In particular, the plasma chemistry, electrical potentials and film surface growth conditions must be duplicated in order to prepare the proper film quality and film microstructure. Specifically, a deposition system which comes close to replicating the plasma densities for all of the Si based radicals and H atoms in the plasma, the substrate self bias and the plasma potential, and the electron and ion bombardment of the growth surface must be designed. Only when this is done will one have the potential of achieving the high efficiencies with the large area systems. While the present internal hardware design for the 5MW chambers is not dramatically different from the design for the small scale systems used to prepare the high efficiency cells, a design for the large area chamber internal hardware which more accurately reproduces the small scale geometry might lead to higher large area cell efficiencies.

Objective of Cathode Hardware Studies

In this program, we will develop new internal hardware for the i-layer deposition chambers used in United Solar's 5MW production line in order to improve the quality and uniformity of these materials to increase the overall solar cell and machine efficiencies. Three newly designed cathodes will be built, tested and compared with the 5MW design during this three year program. To judge how usefulness of each design, single-layers are being made to test the ability to obtain uniform deposits over large areas and large regions of deposition parameter space while single-junction a-Si:H cells are being fabricated to test the quality of the deposited layers. Each design is first tested in a single chamber system with a static substrate.

Once final designs for the internal hardware are completed, the hardware is to be incorporated into an existing chamber on the 2 MW pilot semiconductor line at United Solar (see Figure 30). To test this new internal hardware, single-junction nip a-Si:H cells will be prepared using the new hardware on a moving web substrate. The i-layer conditions will be optimized for the highest FF for cells with similar J_{sc} values. Improvements in the hardware will be judged by increased FF for the cells and improved deposition uniformity over those obtained with the 5MW style cathodes. If necessary, alterations to the system hardware will be made so that the plasma and growth conditions more closely match those for the small area R&D system. Also, temperature, gas flow and pressure distributions throughout the chamber will be closely monitored. If it is demonstrated that this new design is an improvement over the presently used design, we will incorporate the new chamber design into the 5MW production line.

Fig. 30. Double-junction roll-to-roll plasma-CVD processor, previously used as United Solar's production machine. This machine will be used as an experimental machine for much of the work proposed in Tasks 1 and 3.

This roll-to-roll PECVD processor was used as a solar cell production machine when United Solar's production plant had a capacity of 2 MW. It is capable of making nipnip Tandem solar cell structures on a 14" web. The i-layer cathode lengths vary from 17" to 56" long.

Experimental

Thus far, we have developed three new cathode designs, fully tested one design and will test two others in the later stages of the program. The new designs will incorporate several ideas that were devised during the 5MW machine optimization program, during which a great deal of knowledge was obtained. Further studies of the 5MW cathode design in this program has also proved beneficial towards the development of this new hardware. Incorporation of several improvements should lead to better control of the gas flow, temperature distribution and film uniformity across the cathode and deposition area.

Initial tests of the cathodes are being completed using a single test deposition chamber (see Figure 31) in which two different styles of cathodes can simultaneously be compared in the same environment. During this first year, we designed, built and compared one new cathode design with a cathode that mimics the design used in 5MW production machine. In the same system pump-down, single layer films to test deposition uniformity and/or i-layers for nip solar cells to test i-layer quality were made from both types of cathodes.

Typically, the same deposition conditions were used for both deposits including the same rf power density. For the single layer deposits on bare stainless steel substrates, film thickness across the deposition area was measured using standard optical techniques. The 13.56 MHz Plasma Enhanced Chemical Vapor Deposition (PECVD) technique is being used to deposit all of the materials.

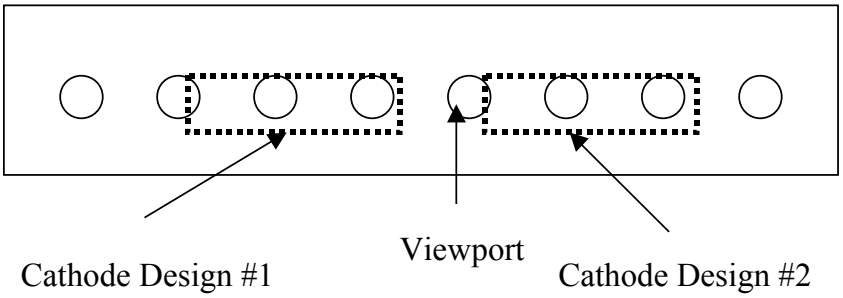

Fig. 31. Single chamber system used for cathode development.

To fabricate 0.25 cm^2 a-Si:H single-junction test cells, the cathode hardware to be tested is only being used to prepare the i-layer materials. Preparation of both the intrinsic layer and the doped layers in a single chamber system is not desirable because of the cross contamination effects which hinder electron and hole collection in the cell. Therefore to make the cells for this study using the single chamber system, we are making the n- and p-layers by the PECVD method in a separate, proven load lock R&D system. This system has prepared high efficiency triple-junction devices in the past and is presently used to make high efficiency single junction cells. The steps we will use to prepare each of the devices are as follows:

1) deposit an a-Si:H:P n-layer using the load lock system,
2) quickly transport the n-layer coated substrates to the single chamber system attempting to minimize air exposure,
3) deposit i-layers using the two different cathode designs,
4) quickly transport the n/i coated substrates from the single chamber system to the load lock system again attempting to minimize air exposure,
5) deposit an a-Si:H:B p-layer using the load lock system,
6) deposit ITO/Al contacts using standard evaporation techniques.

Such a device is depicted in Figure 32. For these studies, we will focus on cells made without current enhancing Ag/ZnO backreflectors to minimize the complexity of the cells.

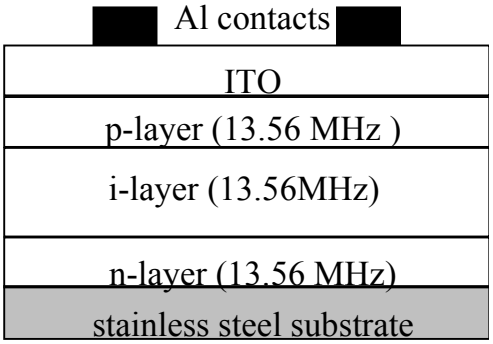

Fig. 32. a-Si:H single-junction cell structure.

In the pilot machine, all three semiconductor layers (n-, i- and p-layers) are being deposited in the roll-to-roll process. Again, these layers are being deposited on bare stainless steel substrates. ITO contacts are deposited using an evaporation technique in a 1 sq. ft. R&D machine while Al contacts are evaporated onto the ITO using a small scale reactor to prepare the 0.25 cm^2 cells.

To characterize the devices, current vs. voltage (IV) measurements are made to obtain standard solar cell device parameters (short circuit current (Jsc), Fill Factor (FF), Open Circuit Voltage (Voc), etc.). Also, quantum efficiency measurements are also used to obtain integrated currents and determine collection losses in cell.

After initial cell measurements, the devices are being subjected to light soaking periods. We are first light soaking the samples for 100 hr under AM1.5 light at 50°C, after each of these periods measuring the cell properties. To measure the stable efficiencies, one must light soak the devices for 600 hrs. But to get preliminary data on how the deposition parameters are affecting the amount of degradation, we are making these limited light exposure measurements to optimize the deposition conditions for minimum degradation and optimum stable cell efficiencies. After initial screen testing, we are selecting certain cells for long term light exposures to obtain accurate values for the stable efficiencies.

Phase II Results

Tests Completed Using The Single Chamber System

The first generation hardware was an improvement in terms of deposition uniformity. There was a problem, however, in that the design changes led to different plasma potentials which led to poorer cell performance, in particular, lower fill factors.

With the second generation hardware, we altered the cathode design in order to achieve the desired electrical properties for the plasma. Figure 33 shows that, like the first generation hardware, we are able to obtain uniform deposition over a large section of the cathode area. In the figure, the deposition rate at various positions above the cathode is plotted across the cathode length. The deposition rate varies little over the length of the cathode even at relatively high deposition rates of 3.9 Å/s where the rate varies by ±6% (see figure).

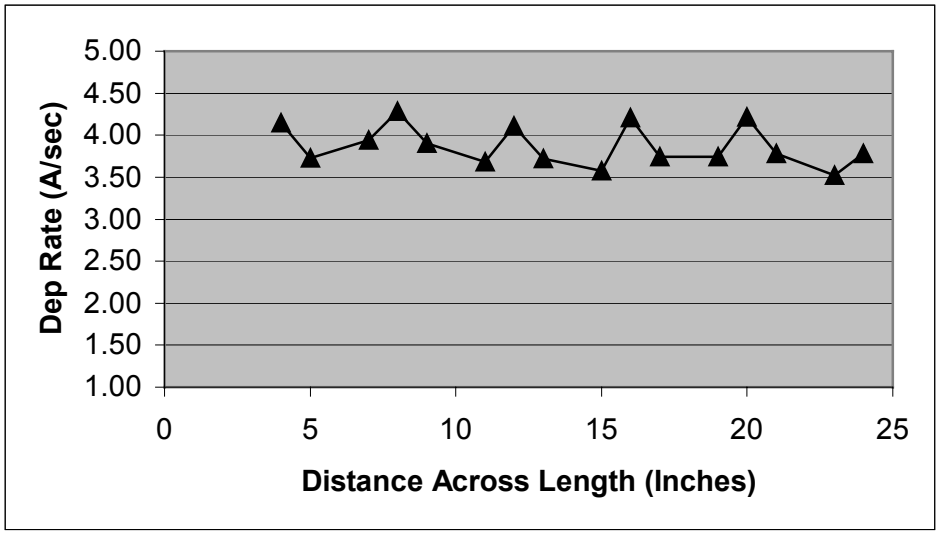

Fig. 33. Deposition rate vs. position along the cathode in the 2nd generation system.

Using this cathode hardware and the single chamber system (see Figure 31) for a-Si:H i-layer depositions, nip cell have been fabricated. In Table VI, data for these cells is compared with data for cells made using the 1st generation hardware and the single chamber system to prepare the i-layers. Cells with similar i-layer thicknesses (near 1500Å) and i-layer deposition rates are compared. One can see that the performance of this 2nd generation hardware is superior to that for the 1st generation hardware demonstrating a significant improvement. The cell efficiency (P_{max}) is higher due to a better fill factor (FF). These results encouraged us to test this new hardware design in the pilot roll-to-roll machine at United Solar where there would be no air break between doped and i-layer depositions.

Table VI. Comparison of performance of cells produced in the 1st and 2nd generation cathode hardware.

Cathode	V_{oc} (V)	J_{sc} (mA/cm^2)	FF	R_s (ohm cm^2)	P_{max} (mW/cm^2)
1st generation	**0.950**	**9.02**	**0.660**	**13.7**	**5.66**
2nd generation	**0.947**	**9.00**	**0.696**	**9.5**	**5.93**

Tests in the Pilot Roll-to-Roll Machine

In this Phase II program, the 2nd and 3rd generation of cathode hardware were installed into and initially tested in the pilot roll-to-roll machine. As mentioned previously, the film uniformity for the 2nd generation hardware was tested in a static mode using the single chamber system (results previously discussed). In contrast, no such tests were made of the 3rd generation hardware prior to installation into the roll-to-roll processor. From the experience gained from the hardware testing already completed, it was felt that the probability of success with this 3rd generation hardware was high and that testing in the moving web system should be expedited.

Figure 34 displays two deposition rate profiles for a-Si:H films across the cathode length for the 3rd generation hardware. This data was obtained with the web in a static mode using the pilot roll-to-roll machine. Again, the deposition rate calculated from the film thicknesses over different position of the cathode is shown in the figure. The top profile is for an a-Si:H film prepared at a rate of 2.9 Å/s while the second is for an a-SiGe:H film made at 4.3 Å/s. At the rates of 2.9 and 4.3 A/s, these values are respectively 1.5 and 2.2 larger than the rate used in production**.** From this data, one can see that with the 3rd generation hardware, the goal of ± 5% thickness uniformity across 80% of the cathode areas has been achieved at deposition rates that are 1.5 and 2 times larger than those used in production. It is particularly important that this goal was achievable for the a-SiGe:H alloy.

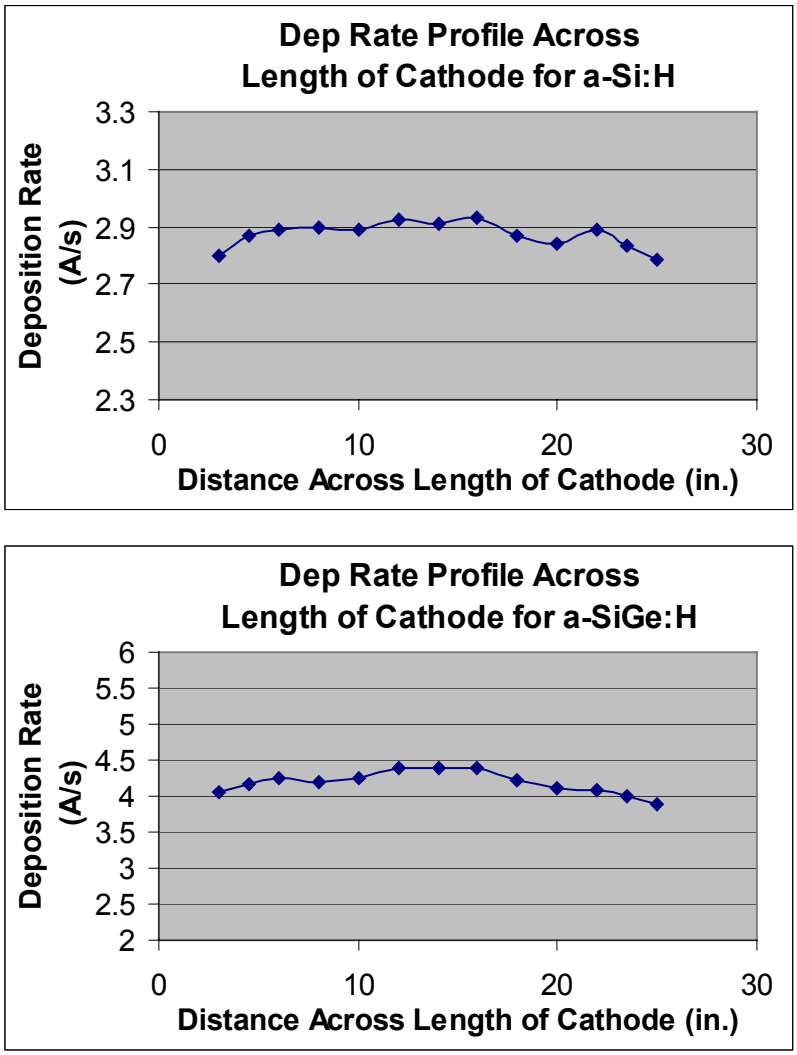

Fig. 33. Deposition rate vs. position along the cathode in the 3rd generation system.

In Table VII, data for a-Si:H cells made using the 2nd and 3rd generation hardware in the pilot line are compared with data for a-Si:H cells made using the 5MW production line. All the cells were made without current enhancing back reflector layers and the ITO/Al contacts were made using small R&D evaporators. The i-layer thicknesses for the cells listed in the table are similar (near 1000 Å) as were the i-layer deposition rates. The doped-layers were made in the same roll-to-roll pilot deposition line used to make the i-layers. Thus, for each cathode hardware, the nip semiconductor stack was made in a true roll-to-roll manner. From the data in the table, it is clear that the cell made using the third generation hardware outperform those made using the 2nd generation hardware. Also, the performance of these cells is superior to that for cells made using the standard 5 MW cathode hardware. In fact, the cell efficiencies obtained using the 3rd generation hardware are 4% higher than those made using the 5 MW cathode hardware with an excellent fill factor of 0.75. Thus, we were able to achieve the phase II goal of a 3% increase in cell performance. Also, this 4% improvement was made without a full

optimization of all the conditions used to make the i-layer. Thus, even better performance should come through systematic optimization of the deposition conditions.

In the next year we plan on further optimization of the 3rd generation cathode hardware and the deposition conditions used to make the i-layers with this hardware to achieve the program goal of a 6% improvement in cell performance.

Table VII. Comparison of performance of cells produced in the 2nd and 3rd generation hardware to cells produced in the 5 MW style hardware.

Cathode	V_{oc} (V)	J_{sc} (mA/cm^2)	FF	R_s (ohm cm^2)	P_{max} (mW/cm^2)
2nd generation	**0.947**	**7.2**	**0.727**	**9.7**	**4.96**
3rd generation	**0.980**	**7.86**	**0.753**	**8.1**	**5.80**
5MW	**0.968**	**7.90**	**0.724**	**8.1**	**5.60**

Phase III Plans

In Phase III we will continue our studies of different cathode hardware using the pilot roll-to-roll line. In order to achieve the program goal of a 6% improvement in cell performance, the deposition conditions used to make cells with the 3rd generation hardware will be further optimized. The deposition conditions to be optimized include the substrate temperature, the gas flows, pressure and applied power. If required, we will also make small modifications to the cathode hardware itself to improve the cell performance. However, with a full optimization study of the deposition conditions with the existing 3rd generation hardware, achievement of the 6% improvement in performance should be possible.

TASK 8A – DEVELOPMENT OF PINCH VALVE TECHNOLOGY

Summary

This portion of the PVMat Program has been extremely successful – the milestone for testing this device in United Solar's 5 MW production machine was scheduled for early in the Phase III portion of the program. This milestone has already been achieved in Phase II. In Phase III we shall undertake the vacuum, interlock, and sequence of operations changes necessary to put this system into operation. At that time, the turnaround time in the a-Si deposition machine, the production rate limiting machine, will be reduced by 1.5 to 2 hrs, resulting in an immediate throughput increase for this machine, and consequently, the 5 MW production facility. We expect additional benefits in terms of reliability as thermal cycling of the machine will be reduced. These devices are now being used as models to develop new pinch valves for the new United Solar 25 MW production equipment being fabricated by ECD.

Overview

We have developed and installed a sealing mechanism in the pay-off and take-up chambers of United Solars roll-to-roll a-Si vacuum deposition production machine that makes a reliable vacuum seal around the 5 mil (127 μm) thick stainless steel substrate. This pinch valve will allow production coil changes to be made while the process chambers remained under vacuum. It is estimated that as much as two hours might be saved at turn around between production runs with the use of this device by eliminating the cool-down and heat-up periods; in addition, the process chambers would not be exposed to atmosphere resulting in lower contamination levels. We expect that the reduction in the number of heat-up and cool-down cycles may also increase the lifetime of components in the machines.

The first step in the development process required the fabrication of a prototype design with half the valve slot width of the final design. The prototype was then held in a bench vice, with a helium mass spectrometer attached for leak checking the device. A sample of the 5 mil production substrate was placed in the sealing slot and the pinch valve was actuated for several hundred cycles. The results demonstrated that the prototype was able to make a reliable vacuum seal around the substrate, with helium leak through rates between 2×10^{-10} and 2×10^{-8} sccm. This was convincing proof of the design concept, so the scale up design work was carried out.

Once the final design and fabrication of the pinch valves was completed, the same bench testing procedures were carried out on these devices as described above. The valves preformed as well as the prototype and they where then installed in the pay-off and take-up chambers. The pinch valves where tested in the production system by venting only the pay-off and the take-up chambers and checking the valve leak through with the helium mass spectrometer.

The result was the pinch valve on the pay-out chamber sealed around the substrate with no detectable leak; a leak in the 10^{-8} sccm range was detected at the take-up side valve – a level two orders of magnitude below the tolerable level. Consequently, both valves preformed to specification.

A description of the valve design and its principles of operation follows. The seal design incorporates the use of a special gasket material that is affixed to sealing the surfaces, (one static [above], and one dynamic [below]). The dynamic surface is actuated by a cam mechanism and is suspended from this mechanism with die springs that can be adjusted to increase or decrease the seal face pressure as required to make a reliable seal. The static seal surface incorporates a special seal that the web passes through; the seal allows for a vacuum seal to be made all way around the slot.

The pinch valve uses material and methods of construction acceptable to ultra-high purity vacuum practice. All the moving parts utilize needle bearings with a very high load bearing capability. We expect that the device should have a projected life in excess of the processor itself.

REPORT DOCUMENTATION PAGE

Form Approved
OMB NO. 0704-0188

1. AGENCY USE ONLY (Leave blank)	2. REPORT DATE	3. REPORT TYPE AND DATES COVERED
	December 2000	Phase II Annual Subcontract Technical Report, June 1999 – August 2000

4. TITLE AND SUBTITLE
Efficiency and Throughput Advances in Continuous Roll-to-Roll a-Si Alloy PV Manufacturing Technology; Phase II Annual Subcontract Technical Report, June 1999 – August 2000

5. FUNDING NUMBERS
C: ZAX-8-17647-09
TA: PVP16101

6. AUTHOR(S)
T. Ellison

7. PERFORMING ORGANIZATION NAME(S) AND ADDRESS(ES)
Energy Conversion Devices, Inc.
1675 W Maple Rd.
Troy MI 48084

8. PERFORMING ORGANIZATION REPORT NUMBER

9. SPONSORING/MONITORING AGENCY NAME(S) AND ADDRESS(ES)
National Renewable Energy Laboratory
1617 Cole Blvd.
Golden, CO 80401-3393

10. SPONSORING/MONITORING AGENCY REPORT NUMBER
NREL/SR-520-29288

11. SUPPLEMENTARY NOTES
NREL Technical Monitor: R.L. Mitchell

12a. DISTRIBUTION/AVAILABILITY STATEMENT
National Technical Information Service
U.S. Department of Commerce
5285 Port Royal Road
Springfield, VA 22161

12b. DISTRIBUTION CODE

13. *ABSTRACT* (Maximum 200 words) This report describes the project by Energy Conversion Devices, Inc. (ECD) and its American joint venture, United Solar Systems Corp. (United Solar), to develop and commercialize a roll-to-roll triple-junction amorphous silicon alloy PV manufacturing technology. This low material cost, roll-to-roll production technology has the economies of scale to meet the cost goals necessary for widespread use of PV. ECD developed and built the present 5-MW United Solar manufacturing plant in Troy, Michigan, and is now designing and building a new 25-MW facility, also in Michigan. United Solar holds the world's record for amorphous silicon PV conversion efficiency, and manufactures and markets a wide range of PV products including flexible portable modules, power modules, and innovative building-integrated PV (BIPV) shingle and metal-roofing modules that take advantage of this lightweight, rugged, and flexible PV technology. All of United Solar's power and BIPV products are approved by Underwriters Laboratories and carry a 10-year warranty.

ECD and United Solar are addressing issues to reduce the cost and to improve the manufacturing technology for the ECD/United Solar PV module manufacturing process. ECD and United Solar identified five technology development tasks that would reduce the module manufacturing cost in the present 5-MW production facility and would also be applicable to future larger-scale manufacturing facilities. These development tasks are: Task 5: Improved substrate heating and monitoring systems; Task 6: The development of new on-line diagnostic systems; Task 7: Development of new back-reflector deposition technology; Task 8: Development of improved RF PECVD reactor cathode and gas distribution configurations; and Task 8A: Development of new pinch valve technology.

14. SUBJECT TERMS
photovoltaics ; roll-to-roll production ; triple junction ; amorphous silicon ; PV conversion efficiency ; substrate heating and monitoring systems ; on-line diagnostic systems ; back-reflector deposition ; RF PECVD reactor cathode ; gas distribution configurations ; pinch valve ; PVMaT

15. NUMBER OF PAGES

16. PRICE CODE

17. SECURITY CLASSIFICATION OF REPORT	18. SECURITY CLASSIFICATION OF THIS PAGE	19. SECURITY CLASSIFICATION OF ABSTRACT	20. LIMITATION OF ABSTRACT
Unclassified	Unclassified	Unclassified	UL